

1
2
3
4
5
6
7
8
9
10
11
12
13
14
15
16
17
18
19
20
21

**ICE, CLOUD, and Land Elevation Satellite-2
(ICESat-2) Project**

**Algorithm Theoretical Basis Document (ATBD)
For
Land-Ice Along-Track Products Part 2:
Land-ice H(t)/ATL11**

**Prepared By: Benjamin Smith, Suzanne Dickinson, Benjamin Jelley,
Tom Neumann, David Hancock, Jeffery Lee, Kaitlin Harbeck**



**Goddard Space Flight Center
Greenbelt, Maryland**

27
28

29

Abstract

30

31

CM Foreword

32 This document is an Ice, Cloud, and Land Elevation Satellite-2 (ICESat-2) Project Science
33 Office controlled document. Changes to this document require prior approval of the Science
34 Development Team ATBD Lead or designee. Proposed changes shall be submitted in the
35 ICESat-II Management Information System (MIS) via a Signature Controlled Request (SCoRe),
36 along with supportive material justifying the proposed change.

37 In this document, a requirement is identified by “shall,” a good practice by “should,” permission
38 by “may” or “can,” expectation by “will,” and descriptive material by “is.”

39 Questions or comments concerning this document should be addressed to:

40 ICESat-2 Project Science Office

41 Mail Stop 615

42 Goddard Space Flight Center

43 Greenbelt, Maryland 20771

44

45

Preface

46 This document is the Algorithm Theoretical Basis Document for the TBD processing to be
47 implemented at the ICESat-2 Science Investigator-led Processing System (SIPS). The SIPS
48 supports the ATLAS (Advance Topographic Laser Altimeter System) instrument on the ICESat-
49 2 Spacecraft and encompasses the ATLAS Science Algorithm Software (ASAS) and the
50 Scheduling and Data Management System (SDMS). The science algorithm software will produce
51 Level 0 through Level 4 standard data products as well as the associated product quality
52 assessments and metadata information.

53 The ICESat-2 Science Development Team, in support of the ICESat-2 Project Science Office
54 (PSO), assumes responsibility for this document and updates it, as required, as algorithms are
55 refined or to meet the needs of the ICESat-2 SIPS. Reviews of this document are performed
56 when appropriate and as needed updates to this document are made. Changes to this document
57 will be made by complete revision.

58 Changes to this document require prior approval of the Change Authority listed on the signature
59 page. Proposed changes shall be submitted to the ICESat-2 PSO, along with supportive material
60 justifying the proposed change.

61 Questions or comments concerning this document should be addressed to:

62 Tom Neumann, ICESat-2 Project Scientist
63 Mail Stop 615
64 Goddard Space Flight Center
65 Greenbelt, Maryland 20771

66

Review/Approval Page

Prepared by:

Benjamin Smith
Principal Researcher
University of Washington
Applied Physics Lab Polar Science Center
1013 NE 40th Street
Box 355640
Seattle, WA 98105

Reviewed by:

Shane Grigsby
Postdoctoral Scholar
Colorado School of Mines
Department of Geophysics

Ellen Enderlin
Assistant Professor
Department of Geosciences
Boise State University

Approved by:

Tom Neumann
<*Enter Position Title Here*>
<*Enter Org/Code Here*>

Change History Log

Revision Level	Description of Change	Date Approved
1.0	Initial Release	

71

List of TBDs/TBRs

Item No.	Location	Summary	Ind./Org.	Due Date

72

73	Table of Contents		
74	Abstract		ii
75	CM Foreword		iii
76	Prefaceiv		
77	Review/Approval Page		v
78	Change History Log		vi
79	List of TBDs/TBRs		vii
80	Table of Contents.....		viii
81	List of Figures		x
82	List of Tables.....		xi
83	1.0 INTRODUCTION.....		1
84	2.0 BACKGROUND INFORMATION and OVERVIEW		2
85	2.1 Background		2
86	2.1.1 Repeat and non-repeat cycles in the ICESat-2 mission		3
87	2.2 Physical Basis of Measurements / Summary of Processing		6
88	2.3 Description of the ATL 11: Land Ice H (t) product.....	Error! Bookmark not	
89	defined.		
90	3.0 ALGORITHM THEORY: Derivation of Land Ice H (t)/ATL11 (L3B).....		8
91	3.1 Elevation-correction Coordinate Systems		3
92	3.2 Input data editing		10
93	3.2.1 Input data editing using ATL06 parameters		11
94	3.2.2 Input data editing by slope		12
95	3.2.3 Spatial data editing		13
96	3.3 Reference-Surface Shape Correction		14
97	3.3.1 Reference-surface shape inversion		14
98	3.3.2 Misfit analysis and iterative editing		15
99	3.4 Reference-shape Correction Error Estimates		16
100	3.5 Calculating corrected height values for repeats with no selected pairs		17
101	3.6 Calculating systematic error estimates		17
102	3.7 Calculating shape-corrected heights for crossing-track data		18
103	3.8 Calculating parameter averages		19

ICESat-2 Algorithm Theoretical Basis Document (ATBD) for Land Ice H(t) (ATL11)

Release 001

104	3.9	Output data editing.....	19
105	4.0	LAND ICE PRODUCTS: Land Ice H (t)(ATL 11/L3B).....	20
106	4.1	<i>Corrected_h</i> group.....	20
107	4.2	<i>Ref_surf</i> group.....	22
108	4.3	<i>Cycle_stats</i> group.....	24
109	4.4	<i>Crossing_track_data</i> group.....	26
110	5.0	ALGORITHM IMPLEMENTATION.....	28
111	5.1.1	Select ATL06 data for the current center point.....	29
112	5.1.2	Select pairs for the reference-surface calculation.....	29
113	5.1.3	Adjust the fit-point center to include the maximum number of cycles.....	32
114	5.1.4	Calculate the reference surface and corrected heights for selected pairs	33
115	5.1.5	Calculate corrected heights for cycles with no selected pairs.....	36
116	5.1.6	Calculate corrected heights for crossover data points.....	38
117	5.1.7	Provide error-averaged values for selected ATL06 parameters.....	39
118	5.1.8	Provide miscellaneous ATL06 parameters.....	40
119	5.1.9	Characterize the reference surface.....	41
120	6.0	Appendix A: Glossary.....	43
121		Glossary/Acronyms.....	56
122		References.....	58
123			

124
125
126
127
128
129
130
131
132
133
134
135

List of Figures

<u>Figure</u>	<u>Page</u>
Figure 2-1. ICESat-2 repeat-track schematic.....	3
Figure 2-2. ATL06 data for an ATL11 reference point.....	4
Figure 2-3. ATL11 coverage.....	7
Figure 3-1. ATL11 fitting schematic	8
Figure 3-2. Data selection.....	11
Figure 5-1 Flow Chart for ATL11 Surface-shape Corrections.....	28
Figure 6-1. Spots and tracks, forward flight	47
Figure 6-2. Spots and tracks, backward flight	48

136

List of Tables

137

138	<u>Table</u>	<u>Page</u>
139	Table 3-1 Parameter Filters to determine the validity of segments for ATL11 estimates.....	10
140	Table 4-1 Parameters in the <i>/ptx/</i> group.....	21
141	Table 4-2 Parameters in the <i>/ptx/ref_surf</i> group.....	22
142	Table 4-3 Parameters in the <i>/ptx/cycle_stats</i> group.....	24
143	Table 4-4 Parameters in the <i>/ptx/crossing_track_data</i> group.....	26
144		

145 **1.0 INTRODUCTION**

146 This document describes the theoretical basis and implementation of the level-3b land-ice
147 processing algorithm for ATL11, which provides time series of surface heights. The higher-level
148 products, providing gridded height, and gridded height change will be described in supplements
149 to this document available in early 2020.

150 ATL11 is based on the ICESat-2 ATL06 Land-ice Height product, which is described elsewhere
151 (Smith and others, 2019a, Smith and others, 2019b). ATL06 provides height estimates for 40-
152 meter overlapping surface segments, whose centers are spaced 20 meters along each of ICESat-
153 2's RPTs (reference pair tracks) but displaced horizontally both relative to the RPT and relative
154 to one another because of small (a few tens of meters or less) imprecisions in the satellite's
155 control of the measurement locations on the ground. ATL11 provides heights corrected for these
156 offsets between the reference tracks and the location of the ATLAS measurements. It is intended
157 as an input for high-level products, ATL14 and ATL15, which will provide gridded estimates of
158 ice-sheet height and height change, but also may be used alone, as a spatially-organized product
159 that allows easy access to height-change information derived from ICESat-2.

160 ATL11 employs a technique which builds upon those previously used to measured short-term
161 elevation changes using ICESat repeat-track data. Where surface slopes are small and the
162 geophysical signals are large compared to background processes (i.e., ice plains and ice shelves),
163 some studies have subtracted the mean from a collection of height measurements from the same
164 repeat track to leave the rapidly-changing components associated with subglacial water motion
165 (Fricker and others, 2007) or tidal flexure (Brunt and others, 2011). In regions where off-track
166 surface slopes are not negligible, height changes can be recovered if the mean height and an
167 estimate of the surface slope (Smith and others, 2009) are subtracted from the data, although in
168 these regions the degree to which the surface slope estimate and the elevation-change pattern are
169 independent is challenging to quantify.

170 ICESat-2's ATL06 product provides both surface height and surface-slope information each time
171 it overflies its reference tracks. The resulting data are similar to that from the scanning laser
172 altimeters that have been deployed on aircraft in Greenland and Antarctica for two decades
173 (cite), making algorithms originally developed for these instruments appropriate for use in
174 interpreting ATLAS data. One example is the SERAC (Surface Elevation Reconstruction and
175 Change Detection) algorithm (Schenk & Csatho, 2012) provides an integrated framework for the
176 derivation of elevation change from altimetry data. In SERAC, polynomial surfaces are fit to
177 collections of altimetry data in small (< 1 km) patches, and these surfaces are used to correct the
178 data for sub-kilometer surface topography. The residuals to the surface then give the pattern of
179 elevation change, and polynomial fits to the residuals as a function of time give the long-term
180 pattern of elevation change. The ATL11 algorithm is similar to SERAC, except that (1)
181 polynomial fit correction is formulated somewhat differently, so that the ATL11 correction gives
182 the surface height at the fit center, not the height residual, and (2) ATL11 does not include a
183 polynomial fit with respect to time.

184

185 **2.0 BACKGROUND INFORMATION AND OVERVIEW**

186 This section provides a conceptual description of ICESat-2’s ice-sheet height measurements and
187 gives a brief description of the derived products.

188 **2.1 Background**

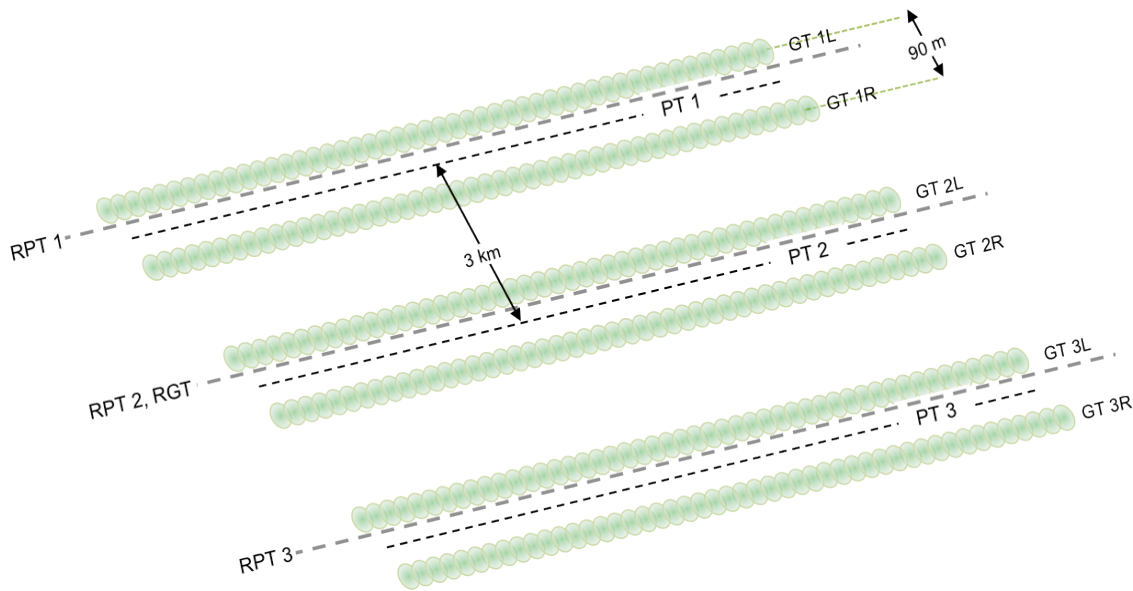
189 The primary goal of the ICESat-2 mission is to estimate mass-balance rates for the Earth’s ice
190 sheets. An important step in this process is the calculation of height change at specific locations
191 on the ice sheets. In an ideal world, a satellite altimeter would exactly measure the same point
192 on the earth on each cycle of its orbit. However, there are limitations in a spacecraft’s ability to
193 exactly repeat the same orbit and to point to the same location. These capabilities are greatly
194 improving with technological advances but still have limits that need to be accounted for when
195 estimating precise elevation changes from satellite altimetry data. The first ICESat mission
196 allowed estimates of longer-term elevation rates using along-track differencing, because
197 ICESat’s relatively precise (50-150-m) pointing accuracy, precise (4-15 m) geolocation
198 accuracy, and small (35-70-m) footprints allowed it to resolve small-scale ice-sheet topography.
199 However, because ICESat had a single-beam instrument, its repeat-track measurements were
200 reliable only for measuring the mean rate of elevation change, because shorter-term height
201 differences could be influenced by the horizontal dispersion of tracks on a sloping surface.

202 ICESat-2 makes repeat measurements over a set of 1387 reference ground tracks (RGTs),
203 completing a *cycle* over all of these tracks every 91 days. ICESat-2’s ATLAS instrument
204 employs a split-beam design, where each laser pulse is divided six separate beams. The beams
205 are organized into three *beam pairs*, with each separated from its neighbors by 3.3 km (**Figure**
206 **2-1**), each pair following a reference pair track (RPT) that is parallel to the RGT. The beams
207 within each pair separated by 90 m, which means that each cycle’s measurement over an RPT
208 can determine the surface slope independently, and a height difference can be derived from
209 any two measurements of an RPT. The 90-m spacing between the laser beams in each pair
210 is equal to twice the required RMS accuracy with which ICESat-2 can be pointed at its RPTs,
211 which means that for most, but not all, repeat measurements of a given RPT, the pairs of
212 beams will overlap one another. To obtain a record of elevation change from the collection
213 of paired measurements on each RPT, some correction is still necessary to account for the
214 effects of small-scale surface topography around the RPT in the ATL06 surface heights that
215 appear as a result of this non-exact pointing. ATL11 uses a polynomial fit to the ATL06
216 measurements to correct for small-scale topography effects on surface heights that result
217 from this non-exact pointing.

218 The accuracy of ICESat-2 measurements depends on the thickness of clouds between the
219 satellite and the surface, on the reflectance, slope, and roughness of the surface, and on
220 background noise rate which, in turn, depends on the intensity of solar illumination of the
221 surface and the surface reflectance. It also varies from laser beam to beam, because in each
222 of ICESat-2’s beam pairs one beam (the “strong beam”) has approximately four times the
223 signal strength of the other (the “weak beam”). Parameters on the ATL06 product allow
224 estimation of errors in each measurement and allow filtering of most measurements with

225 large errors due to misidentification of clouds or noise as surface returns (blunders), but to
 226 enable higher precision surface change estimates, ATL11 implements further self-
 227 consistency checks that further reduce the effects of errors and blunders.
 228

Figure 2-1. ICESat-2 repeat-track schematic



Schematic drawing showing the pattern made by ATLAS’s 6-beam configuration on the ground, for a track running from lower left to upper right. The 6 beams are grouped into 3 beam pairs with a separation between beams within a pair of 90m and a separation between beam pairs of 3.3 km. The RPTs (Reference Pair Tracks, heavily dashed lines in gray) are defined in advance of launch; the central RPT follows the RGT (Reference Ground Track, matching the nadir track of the predicted orbit). The Ground Tracks are the tracks actually measured by ATLAS (GT1L, GT1R, etc., shown by green footprints). Measured Pair Tracks (PTs, smaller dashed lines in black) are defined by the centers of the pairs of GTs, and deviate slightly from the RPTs because of inaccuracies in repeat-track pointing. The separation of GTs in each pair in this figure is greatly exaggerated relative to the separation of the PTs.

229 **2.2 Elevation-correction Coordinate Systems**

230 We perform ATL11 calculations using the along-track coordinate system described in the
 231 ATL06 ATBD (Smith and others, 2019b, Smith and others, 2019a). The along-track coordinate
 232 is measured parallel to the RGT, starting at each RGT’s origin at the equator. The across-track
 233 coordinate is measured to the left of the RGT, so that the two horizontal basis vectors and the
 234 local vertical vector form a right-handed coordinate system.

235 **2.3 Terminology:**

236 Some of the terms that we will use in describing the ATL11 fitting process and the data
237 contributing are:

238 *RPT*: Reference pair track

239 *Cycle*: ICESat-2 has 1387 distinct reference ground tracks, which its orbit covers every 91 days.
240 One repeat measurement of these reference ground tracks constitutes a cycle.

241 *ATL06 segment*: A 40-meter segment fit to a collection of ATL03 photon-event data, as
242 described in the ATL06 ATBD

243 *ATL06 pair*: Two ATL06 segments from the same cycle with the same *segment_id*. By
244 construction, both segments in the ATL06 pair have the same along-track coordinate, and are
245 separated by the beam-to-beam spacing (approximately 90 m) in the across-track direction

246 *ATL11 RPT point*: The expected location of each ATL11 point on the RPT, equivalent to the
247 beginning of every third geosegment on the RPT, or the center of every third ATL06 segment.

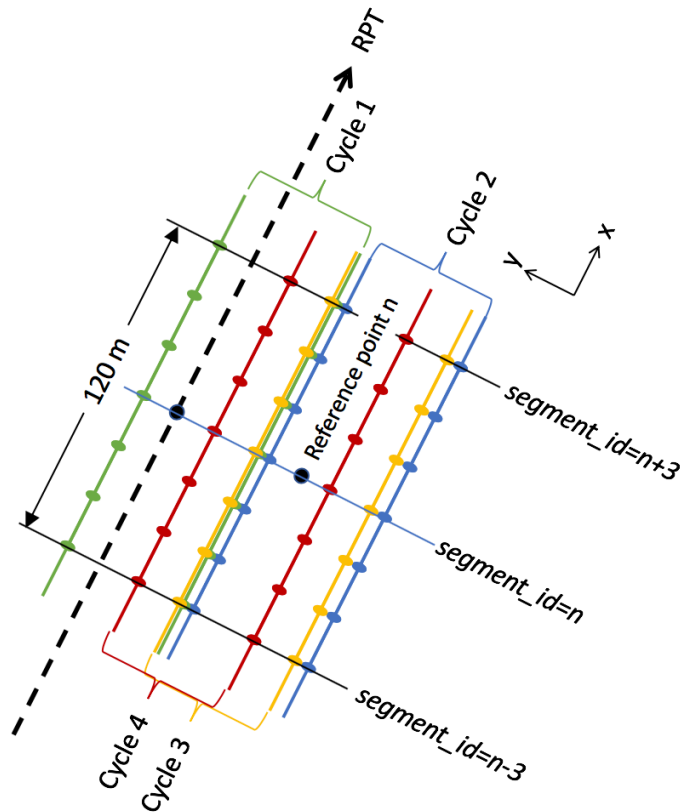
248 *ATL11 reference point*: an *ATL11 RPT point* shifted in the across-track direction to better match
249 the geometry of the available ATL06 data.

250 *ATL11 fit*: The data and parameters associated with a single ATL11 reference point. This
251 includes corrected heights from all available cycles

252

253 ATL11 calculates elevations and elevation differences based on collections of segments from the
254 same beam pair but from different cycles. ATL11 is posted every 60 m, which corresponds to
255 every third ATL06 *segment_id*, and includes ATL06 segments spanning three segments before
256 and after the central segment, so that the ATL11 uses data that span 120 m in the along-track
257 direction. ATL11 data are centered on *reference points*, which has the same along-track
258 coordinate as its central ATL06 segment, but is displaced in the across-track direction to better
259 match the locations of the ATL06 measurements from all of the cycles present (see section
260 3.1.3).

Figure 2-2. ATL06 data for an ATL11 reference point



Schematic of ATL06 data for an ATL11 reference point centered on segment n , based on data from four cycles. The segment centers span 120 m in the along-track data, and the cycles are randomly displaced from the RPT in the across-track direction. The reference point has an along-track location that matches that of segment n , and an across-track position chosen to match the displacements of the cycles.

261

262 2.4 Repeat and non-repeat cycles in the ICESat-2 mission

263 In the early part of the ICESat-2 mission, an error in the configuration of the start trackers
 264 prevented the instrument from pointing precisely at the RGTs. As a result, all data from cycles 1
 265 and 2 were measured between one and two kilometers away from the RGTs, with offsets that
 266 varied in time and as a function of latitude. The measurements from cycles 1 and 2 still give
 267 high-precision measurements of surface height, but repeat-track measurements from ICESat-2
 268 begin during cycle 3, in April of 2019. ATL11 files will be generated for ATL06 granules from
 269 cycles 1 and 2, but these will contain only one cycle of data, plus crossovers, because the
 270 measurements from these cycles (which are displaced from the RPTs by several kilometers) will
 271 not be repeated. We expect the measurements from cycles 1 and 2 to be useful as a reduced-
 272 resolution (compared to ATL06) mapping of the ice sheet, which may prove useful in DEM
 273 generation and in comparisons with other altimetry missions. For cycles 3 and after, each

274 ATL11 granule will contain all available cycles for each RGT (i.e. from cycle 3 onwards), and
275 will contain crossovers between the repeat cycles and cycles 1 and 2.

276 Outside the polar regions, ICESat-2 is pointed to minimize gaps between repeat measurements,
277 and so does not make repeat measurements over its ground tracks. ATL11 is only calculated
278 within the repeat-pointing mask (see Figure ???), which covers areas poleward of 60°N and
279 60°S.

280

281 **2.5 Physical Basis of Measurements / Summary of Processing**

282 Surface slopes on the Antarctic and Greenland ice sheets are generally small, with magnitudes
283 less than two degrees over 99% of Antarctica’s area. Smaller-scale (0.5-3 km) undulations,
284 generated by ice flow over hilly or mountainous terrain may have amplitudes of up to a few
285 degrees. Although we expect that the surface height will change over time, slopes and locations
286 of these smaller-scale undulation are likely controlled by underlying topography and should
287 remain essentially constant over periods of time comparable with the expected 3-7 duration of
288 the ICESat-2 mission. This allows us to use estimates of ice-sheet surface shape derived from
289 data spanning the full mission to correct for small (<130-m) differences in measurement
290 locations between repeat measurements of the same RPT, to produce records of height change
291 for specific locations. To account for changes in the ice-sheet surface slope associated with
292 gradients in thinning, we also solve for the rate of surface-slope change, when sufficient data are
293 available. Further, we can use the surface slope estimates in ATL06 to determine whether
294 different sets of measurements for the same fit center are self-consistent: We can assume that if
295 an ATL06 segment shows a slope significantly different from others measured near the same
296 reference point it likely is in error. The combination of parameters from ATL06 and these self-
297 consistency checks allows us to generate time series based on the highest-quality measurements
298 for each reference point, and our reference surface calculation lets us correct for small-scale
299 topography and to estimate error magnitudes in the corrected data.

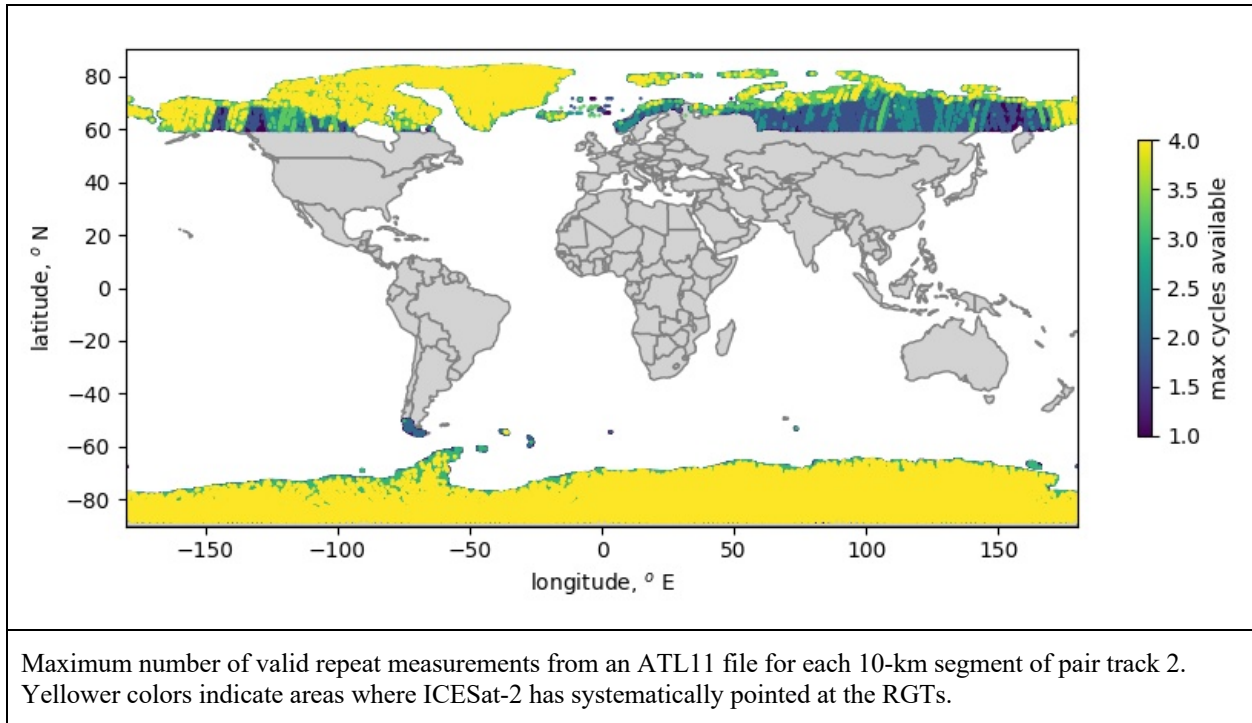
300 **2.5.1 Choices of product dimensions**

301 We have chosen a set of dimensions for the ATL11 fitting process with the goal of creating a
302 product that is conveniently sized for analysis of elevation changes, while still capturing the
303 details of elevation change in outlet glaciers. The assumption that ice-sheet surface can be
304 approximated by a low-degree polynomial becomes untenable as data from larger and larger
305 areas are included in the calculation; therefore we use data from the smallest feasible area to
306 define our reference surface, while still including enough data to reduce the sampling error in the
307 data and to allow for the possibility that at least one or two will encounter a flat surface, which
308 greatly improves the chances that each cycle will be able to measure surface comparable to one
309 another. Each ATL11 point uses data from an area up to 120 m in the along-track direction by
310 up to 130 m in the across-track direction. We have chosen the cross-track search distance
311 ($L_{\text{search_XT}}$) to be 65 m, approximately equal to half the beam spacing, plus three times the
312 observed 6.5 m standard deviation of the across-track pointing accuracy for cycles 3 and 4 in
313 Antarctica. We chose the across-track search distance ($L_{\text{search_AT}}$) to be 60 m, approximately

314 equal to $L_{\text{search_XT}}$, so that the full $L_{\text{search_AT}}$ search window spans three ATL06 segments before
 315 and after the central segment for each reference point. The resulting along-track resolution is
 316 around one third that of ATL06, but still allows 6-7 distinct elevation-change samples across a
 317 small (1-km) outlet glacier.

318 **2.6 Product coverage**

Figure 2-3. Potential ATL11 coverage



319 Over the vegetated parts of the Earth, ICESat-2 makes spatially dense measurements, measuring
 320 tracks parallel to the reference tracks in a strategy that will eventually measure global vegetation
 321 with a track-to-track spacing better than 1 km. Because ATL11 relies upon repeat measurements
 322 over reference tracks to allow the calculation of its reference surfaces, ATL11 is generated for
 323 ICESat-2 subregions 3-5 and 10-12 (global coverage, north and south of 60 degrees). Repeat
 324 measurements are limited to Antarctica, Greenland, and the High Arctic islands (Figure 2-3),
 325 although in other areas the fill-in strategy developed for vegetation measurements allows some
 326 repeat measurements. In regions where ICESat-2 was not pointed to the repeat track, most
 327 ATL11 reference points will provide one measurement close to the RPT. Crossover data are
 328 available for many of these points, though their distribution in time is not regular. A future
 329 update to the product may provide crossover measurements for lower-latitude areas, but the
 330 current product format is not designed to allow this.

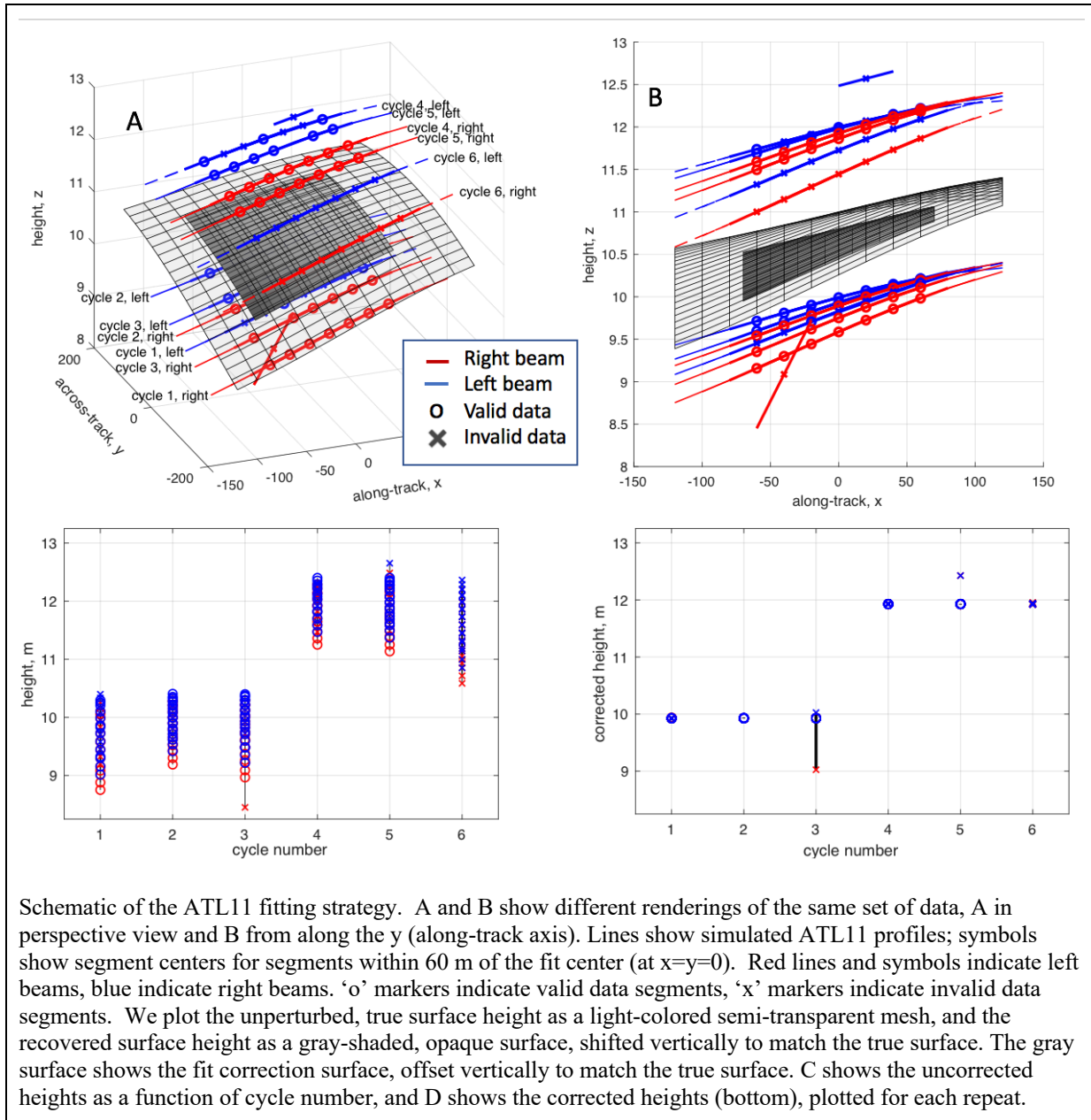
331 **3.0 ALGORITHM THEORY: DERIVATION OF LAND ICE H (T)/ATL11 (L3B)**

332 In this section, we describe in detail the algorithms used in calculating the ATL11 land-ice
333 parameters. This product is intended to provide time series of surface heights for land-ice and
334 ice-shelf locations where ICESat-2 operates in repeat-track mode (*i.e.* for polar ice), along with
335 parameters useful in determining whether each height estimate is valid or a result of a variety of
336 potential errors (see ATL06 ATBD, section 1).

337 ATL11 height estimates are generated by correcting ATL06 height measurements for the
338 combined effects of short-scale (40-120-m) surface topography around the fit centers and small
339 (up to 130-m) horizontal offsets between repeat measurements. We fit a polynomial reference
340 surface to height measurements from different cycles as a function of horizontal coordinates
341 around the fit centers, and use this polynomial surface to correct the height measurements to the
342 fit center. The resulting values reflect the time history of surface heights at the reference points,
343 with minimal contributions from small-scale local topography.

344 In this algorithm, for a set of reference points spaced every 60 meters along each RPT (centered
345 on every third segment center), we consider all ATL06 segments with centers within 60 m along-
346 track and 65 m across-track of the reference point, so that each ATL11 fit contains as many as
347 seven distinct along-track segments from each laser beam and cycle. We select a subset of these
348 segments with consistent ATL06 slope estimates and small error estimates, and use these
349 segments to define a time-variable surface height and a polynomial surface-shape model. We
350 then use the surface-shape model to calculate corrected heights for the segments from cycles not
351 included in the initial subset. We propagate errors for each of these steps to give formal errors
352 estimates that take into account the sampling error from ATL06, and propagate the geolocation
353 errors with the slope of the surface-shape model to give an estimate of systematic errors in the
354 height estimates.

Figure 3-1. ATL11 fitting schematic



Schematic of the ATL11 fitting strategy. A and B show different renderings of the same set of data, A in perspective view and B from along the y (along-track axis). Lines show simulated ATL11 profiles; symbols show segment centers for segments within 60 m of the fit center (at $x=y=0$). Red lines and symbols indicate left beams, blue indicate right beams. 'o' markers indicate valid data segments, 'x' markers indicate invalid data segments. We plot the unperturbed, true surface height as a light-colored semi-transparent mesh, and the recovered surface height as a gray-shaded, opaque surface, shifted vertically to match the true surface. The gray surface shows the fit correction surface, offset vertically to match the true surface. C shows the uncorrected heights as a function of cycle number, and D shows the corrected heights (bottom), plotted for each repeat.

355

356 Figure 3-1 shows a schematic diagram of the fitting process. In this example, we show simulated
 357 ATL06 height measurements for six 91-day orbital cycles over a smooth ice-sheet surface
 358 (transparent grid). Between cycles 3 and 4, the surface height has risen by 2 m. Two of the
 359 segments contain errors: The weak beam for one segment from repeat 3 is displaced downward
 360 and has an abnormal apparent slope in the x direction, and one segment from repeat 5 is
 361 displaced upwards, so that its pair has an abnormal apparent slope in the y direction. Segments
 362 falling within the across and along-track windows of the reference point (at $x=y=0$ in this plot)
 363 are selected, and fit with a polynomial reference surface (shown in gray). When plotted as a

364 function of cycle number (panel C), the measured heights show considerable scatter but when
 365 corrected to the reference surface (panel D), each cycle shows a consistent height, and the
 366 segments with errors are clearly distinct from the accurate measurements.

367 **3.1 Input data editing**

368 Each ATL06 measurement includes location estimates, along- and across-track slope estimates,
 369 and PE (Photon-Event)-height misfit estimates. To calculate the reference surface using the most
 370 reliable subset of available data, we perform tests on the surface-slope estimates and error
 371 statistics from each ATL06-pair to select a self-consistent set of data. These tests determine
 372 whether each pair of measurements is *valid* and can be used in the reference-shape calculation or
 373 is *invalid*. Segments from invalid pairs may be used in elevation-change calculations, but not in
 374 the reference-shape calculation.

375 A complete flow chart of the data-selection process is shown in Figure 3-2, and the parameters
 376 used to make these selections and their values are listed in Table 3-1.

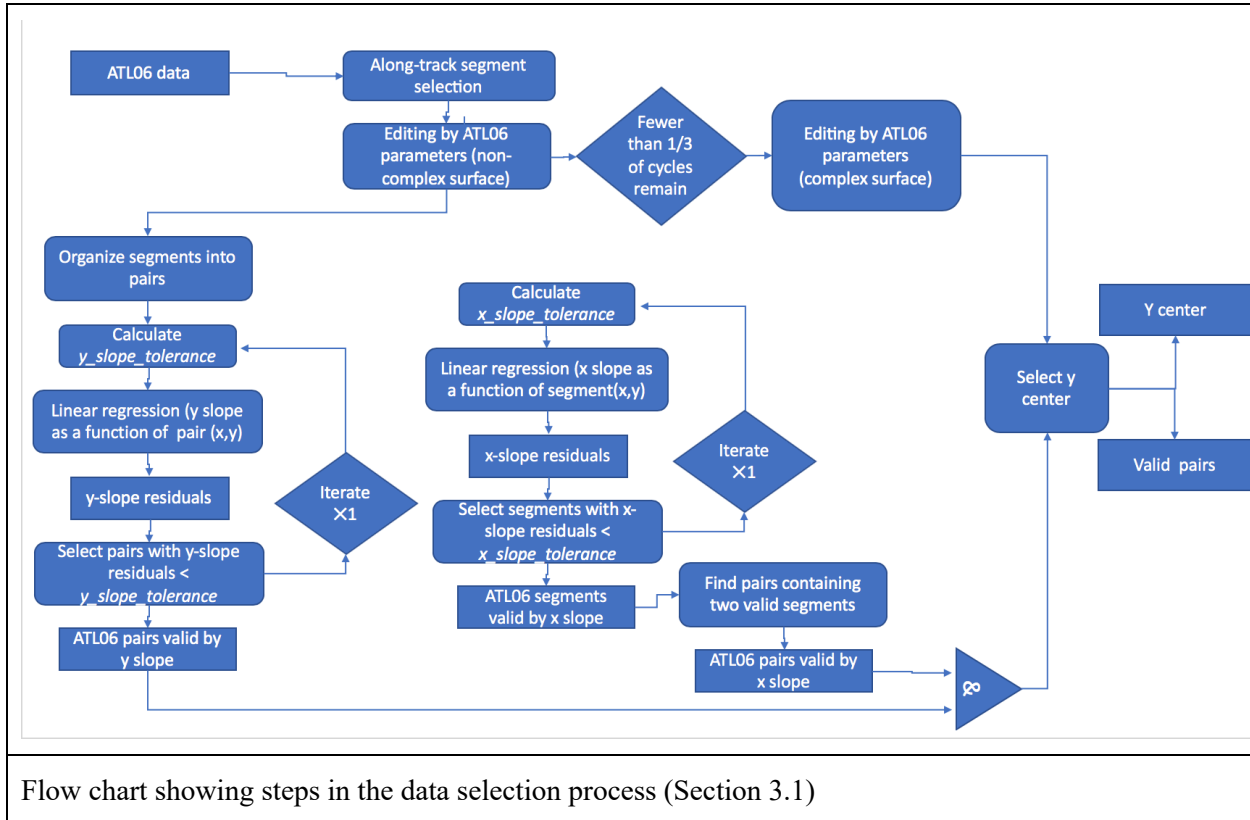
377

378 **Table 3-1 Parameter Filters to determine the validity of segments for ATL11 estimates**

complex_surface_flag	Segment parameter	Filter strategy	Section
0	<i>ATL06_quality_summary</i>	<i>ATL06_quality_summary</i> =0 (indicates high-quality segments)	3.1.1
1	<i>SNR_significance</i>	<i>SNR_significance</i> < 0.02 (indicates low probability of surface-detection blunders)	3.1.1
0 or 1	Along-track differences	Minimum height difference between the endpoints of a segment and the middles of its neighbors must be < 2 m (for smooth surfaces) or < 10 m (for complex surfaces)	3.1.1
0 or 1	<i>h_li_sigma</i>	<i>h_li_sigma</i> < max(0.05, 3*median(<i>h_li_sigma</i>))	3.1.1
0 or 1	Along-track slope	<i>r_slope_x</i> < 3 <i>slope_tolerance_x</i>	3.1.2
0 or 1	Across-track slope	<i>r_slope_y</i> < 3 <i>slope_tolerance_y</i>	3.1.2

0 or 1	Segment location	$ x_{atc}-x_0 < L_{search_XT}$ $ y_{atc}-y_0 < L_{search_AT}$	3.1.3
--------	------------------	----------------------------------------------------------------------	-------

Figure 3-2. Data selection



379

380 3.1.1 Input data editing using ATL06 parameters

381 For each reference point, we collect all ATL06 data from all available repeat cycles that have
 382 *segment_id* values within ± 3 of the reference point (inclusive) and that are on the same *rgt* and
 383 pair track as the reference point. The *segment_id* criterion ensures that the segment centers are
 384 within ± 60 m of the reference point in the along-track direction. We next check that the ATL06
 385 data are close to the pre-defined reference track, by rejecting all ATL06 segments that are more
 386 than 500 m away from the nominal pair across-track coordinates (-3200, 0, and 3200 meters for
 387 right, center, and left pairs, respectively). This removes data that were intentionally or
 388 accidentally collected with ATLAS pointed off nadir (i.e. for calibration scan maneuvers).

389 ATL06 contains some segments with signal-finding blunders (Smith et al., 2019). To avoid
 390 having these erroneous segments contaminate ATL11, we filter using one of two sets of tests,
 391 depending on surface roughness. We identify high-quality ATL06 segments, using parameters
 392 that depend on whether the surface is identified as smooth or rough, as follows:

393 1) For smooth ice-sheet surfaces, we use the ATL06 *ATL06_quality_summary* parameter,
 394 combined with a measure of along-track elevation consistency, *at_min_dh*, that is calculated as
 395 part of ATL11. *ATL06_quality_summary* is based on the spread of the residuals for each
 396 segment, the along-track surface slope, the estimated error, and the signal strength. Zero values
 397 indicate that no error has been found. We define the along-track consistency parameter
 398 *at_min_dh* as the minimum absolute difference between the heights of the endpoints of each
 399 segment and the center heights of the previous and subsequent segments. Its value will be small
 400 if a segment's height and slope are consistent with at least one of its neighbors. For smooth
 401 surfaces, we require that the *at_min_dh* values be less than 2 m. Over smooth ice-sheet surfaces,
 402 the 2-m threshold eliminates most blunders without eliminating a substantial number of high-
 403 quality data points.

404 2) For rough, crevassed surfaces, the smooth-ice strategy may not identify a sufficient number of
 405 pairs for ATL11 processing to continue. If fewer than one third of the original cycles remain
 406 after the smooth-surface criteria are applied, we relax our criteria, using the signal-to-noise ratio
 407 (based on the ATL06 *segment_stats/snr_significance* parameter) to select the pairs to include in
 408 the fit, and require that the *at_min_dh* values be less than 10 m. If we relax the criteria in this
 409 way, we mark the reference point as having a complex surface using the
 410 *ref_surf/complex_surface_flag*, which limits the degree of the polynomial used in the reference
 411 surface fitting to 0 or 1 in each direction.

412 For either smooth or rough surfaces, we perform an additional check using the magnitude of
 413 *h_li_sigma* for each segment. If any segment's value is larger than three times the maximum of
 414 0.05 m and the median *h_li_sigma* for the valid segments for the current reference point, it is
 415 marked as invalid. The limiting 0.05 m value prevents this test from removing high-quality data
 416 over smooth ice-sheet surfaces, where errors are usually small.

417 Each of these tests applies to values associated with ATL06 segments. When the tests are
 418 complete, we check each ATL06 pair (*i.e.* two segments for the same along-track location from
 419 the same cycle) and if either of its two segments has been marked as invalid, the entire pair is
 420 marked as invalid.

421 **3.1.2 Input data editing by slope**

422 The segments selected in 3.1.1 may include some high-quality segments and some lower-quality
 423 segments that were not successfully eliminated by the data-editing criteria. We expect that the
 424 ATL06 slope fields (*dh_fit_dx*, and *dh_fit_dy*) for the higher-quality data should reflect the
 425 shape of an ice-sheet surface with a spatially consistent surface slope around each reference
 426 point, but that at least some of lower-quality data should have slope fields that outliers relative to
 427 this consistent surface slope. In this step, we assume that the slope may vary linearly in *x* and *y*,
 428 and so use residuals between the slope values and a regression of the slope values against *x* and *y*
 429 to identify the data with inconsistent slope values. The data with large residuals are marked as
 430 *invalid*.

431 Starting with valid pairs from 3.2.1, we first perform a linear regression between the *y* slopes of
 432 the pairs and the pair-center *x* and *y* positions. The residuals to this regression define one
 433 *y_slope_residual* for each pair. We compare these residuals against a *y_slope_tolerance*:

$$y_slope_tolerance = \max(0.01, 3 \text{ median } (dh_fit_dy_sigma), 3 \text{ RDE } (y_slope_residuals)) \quad 1$$

434 Here RDE is the Robust Difference Estimator, equal to half the difference between the 16th and
 435 84th percentiles of a distribution, and the minimum value of 0.01 ensures that this test does not
 436 remove high-quality segments in regions where the residuals are very consistent. If any pairs
 437 have a *y_slope_residual* greater than *y_slope_tolerance*, we remove them from the group of valid
 438 pairs, then repeat the regression, recalculate *y_slope_tolerance*, and retest the remaining pairs.

439 We then return to the pairs marked as *valid* from 3.1.1, and perform a linear regression between
 440 the *x* slopes of the segments within the pairs and the segment-center *x* and *y* positions. The
 441 residuals to this regression define one *x_slope_residual* for each segment. We compare these
 442 residuals against an *x_slope_tolerance*, calculated in the same way as (1), except using segment *x*
 443 slopes and residuals instead of pair *y* slopes. As with the *y* regression, we repeat this procedure
 444 once if any segments are eliminated in the first round.

445 After both the *x* and *y* regression procedures are complete, each pair of segments is marked as
 446 *valid* if both of its *x* residuals are smaller than *slope_tolerance_x* and its *y* residual is smaller than
 447 *slope_tolerance_y*.

448 3.1.3 Spatial data editing

449 The data included in the reference-surface fit fall in a “window” defined by a $2L_{search_{XT}}$ by
 450 $2L_{search_{AT}}$ rectangle, centered on each reference point. Because the across-track location of the
 451 repeat measurements for each reference point are determined by the errors in the repeat track
 452 pointing of ATLAS, a data selection window centered on the RPT in the *y* direction will not
 453 necessarily capture all of the available cycles of data. To improve the overlap between the
 454 window and the data, we shift the reference point in the *y* direction so that the window includes
 455 as many valid beam pairs as possible. We make this selection after the parameter-based (3.1.1)
 456 and slope-based (3.1.2) editing steps because we want to maximize the number high-quality pairs
 457 included, without letting the locations of low-quality segments influence our choice of the
 458 reference-point shift.

459 We select the across-track offset for each reference point by searching a range of offset values, δ ,
 460 around the RPT to maximize the following metric:

$$M(\delta) = \frac{[\text{number of unique valid pairs entirely contained in } \delta \pm L_{search_{XT}}] + [\text{number of unpaired segments contained in } \delta \pm L_{search_{XT}}]/100}{2} \quad 2$$

461 Maximizing this metric allows the maximum number of pairs with two valid segments to be
 462 included in the fit, while also maximizing the number of segments included close to the center of
 463 the fit. If multiple values of δ have the same *M* value, we choose the median of those δ values.
 464 The across-track coordinate of the adjusted reference point is then $y_0 + \delta_{max}$, where y_0 is the
 465 across-track coordinate of the unperturbed reference point. After this adjustment, the segments

466 in pairs that are contained entirely in the across-track interval $\delta \pm L_{search\ XT}$ are identified as
 467 *valid* based on the spatial search.

468 The location of the adjusted reference point is reported in the data group for each pair track, with
 469 corresponding local coordinates in the *ref_surf* subgroup: */ptx/ref_surf/x_atc*, */ptx/ref_surf/y_atc*.

470

471 3.2 Reference-Surface Shape Correction

472 To calculate the reference-surface shape correction, we construct the background surface shape
 473 from valid segments selected during 3.1 and 3.2, using a least-squares inversion that separates
 474 surface-shape information from elevation-change information. This produces surface shape-
 475 corrected height estimates for cycles containing at least one valid pair, and a surface-shape
 476 model that we use in later steps (3.4, 3.6) to calculate corrected heights for cycles that contain no
 477 valid pairs and to calculate corrected heights for crossing tracks.

478 3.2.1 Reference-surface shape inversion

479 The reference-shape inversion solves for a reference surface and a set of corrected-height values
 480 that represent the time-varying surface height at the reference point. The inversion involves
 481 three matrices:

482 (i): a polynomial surface shape matrix, **S**, that describes the functional basis for the spatial part of
 483 the inversion:

$$\mathbf{S} = \left[\left(\frac{x - x_0}{l_0} \right)^p \left(\frac{y - y_0}{l_0} \right)^q \right] \quad 3$$

484 Here x_0 and y_0 are equal to the along-track coordinates of the adjusted reference point,
 485 */ptx/ref_surf/x_atc* and */ptx/ref_surf/y_atc*, respectively. **S** has one column for each permutation
 486 of p and q between zero and the degree of the surface polynomial in each dimension, but does
 487 not include a $p=q=0$ term. The degree is chosen to be no more than 3 (in the along-track
 488 direction) or 2 (in the across-track direction), and to be no more than the number of distinct pair-
 489 center y values (in the across-track direction) or more than 1 less than the number of distinct x
 490 values (in the along-track direction) in any cycle, with distinct values defined at a resolution of
 491 20 m in each direction. The scaling factor, l_0 , ensures that the components of **S** are on the order
 492 of 1, which improves the numerical accuracy of the computation. We set $l_0=100$ m, to
 493 approximately match the intra-pair beam spacing.

494 (ii): a matrix that encodes the repeat structure of the data, that accounts for the height-change
 495 component of the inversion:

$$\mathbf{D} = [\delta(i, 1), \delta(i, 2), \dots, \delta(i, N)] \quad 4$$

496 Here δ is the delta function, equal to 1 when its arguments are equal, zero otherwise, and i is an
 497 index that increments by one for each distinct cycle in the selected data.

498 (iii): a matrix that describes the linear rate of change in the surface slope over the course of the
499 mission:

$$\mathbf{S}_t = \left[\left(\frac{x - x_0}{l_0} \right) \left(\frac{t - t_0}{\tau} \right), \left(\frac{y - y_0}{l_0} \right) \left(\frac{t - t_0}{\tau} \right) \right] \quad 5$$

500 Here t_0 is equal to *slope_change_t0*, the mid-point of the mission at the time that ATL11 is
501 generated, halfway between start repeat track pointing (the beginning of cycle 3) and either the
502 end of the mission or the processing time (*slope_change_t0* is an attribute of each ATL11
503 file). This implies that on average, $(t - t_0)$ will have a zero mean. The time-scaling factor, τ , is
504 equal to one year (86400*365.25 seconds). This component will only be included in ATL11
505 once eight complete cycles of data are available on the RGTs (after cycle 10 of the mission).

506 The surface shape, slope change, and height time series are estimated by forming a composite
507 design matrix, \mathbf{G} , where

$$\mathbf{G} = [\mathbf{S} \ \mathbf{S}_t \ \mathbf{D}], \quad 6$$

508 and a covariance matrix, \mathbf{C} , containing the squares of the segment-height error estimates on its
509 diagonal. The surface-shape polynomial and the height changes are found:

$$[\mathbf{s}, \mathbf{s}_t, \mathbf{z}_c] = \mathbf{G}^{-g} \mathbf{z}$$

where

$$\mathbf{G}^{-g} = [\mathbf{G}^T \mathbf{C}^{-1} \mathbf{G}]^{-1} \mathbf{G}^T \mathbf{C}^{-1} \quad 7$$

510 The notation $[\]^{-1}$ designates the inverse of the quantity in brackets, and \mathbf{z} is the vector of segment
511 heights. The parameters derived in this fit are \mathbf{s} , a vector of surface-shape polynomial
512 coefficients, \mathbf{s}_t , the mean rate of surface-slope change, and \mathbf{z}_c , a vector of corrected height values,
513 giving the height at (lat_0, lon_0) as inferred from the height measurements and the surface
514 polynomial. The matrix \mathbf{G}^{-g} is the generalized inverse of \mathbf{G} . The values of \mathbf{s} are reported in the
515 *ref_surf/poly_ref_surf* parameter, as they are calculated from (6), with no correction made for the
516 scaling in (3). The values for the slope-change rates are reported in *ref_surf/slope_change_rate*,
517 after rescaling to units of *years⁻¹*.

518 3.2.2 Misfit analysis and iterative editing

519 If blunders remain in the data input to the reference-surface calculation, they can lead to
520 inaccurate reference surfaces. To help remove these blunders, we iterate the inversion procedure
521 in 3.2.1, eliminating outlying data points based on their residuals to the reference surface.

522 To determine whether outliers may be present, we calculate the chi-squared misfit between the
523 data and the fit surface based on the data covariance matrix and the residual vector, r :

$$\chi^2 = r^T \mathbf{C}^{-1} r \quad 8$$

524 To determine whether this misfit statistic indicates consistency between the polynomial surface
 525 and the data we use a P statistic, which gives the probability that the given χ^2 value would be
 526 obtained from a random Gaussian distribution of data points with a covariance matrix \mathbf{C} . If the
 527 probability is less than 0.025, we perform some further filtering/editing: we calculate the RDE of
 528 the scaled residuals, eliminate any pairs containing a segment whose scaled residual magnitude is
 529 larger than three times that value, and repeat the remaining segments.

530 After each iteration, any column of \mathbf{G} that has a uniform value (i.e. all the values are the same) is
 531 eliminated from the calculation, and the corresponding value of the left-hand side of equation 7
 532 is set to zero. Likewise, if the inverse problem has become less than overdetermined (i.e., the
 533 number of data is smaller than the number of unknown values they are constraining), the
 534 polynomial columns of \mathbf{G} are eliminated one by one until the number of data is greater than the
 535 number of unknowns. Columns are eliminated in descending order of the sum of x and y
 536 degrees, and when there is a tie between columns based on this criterion, the column with the
 537 larger y degree is eliminated first.

538 This fitting procedure is continued until no further segments are eliminated. If more than three
 539 complete cycles that passed the initial editing steps are eliminated in this way, the surface is
 540 assumed to be too complex for a simple polynomial approximation, and we proceed as follows:

541 (i) the fit and its statistics are reported based on the complete set of pairs that passed
 542 the initial editing steps (valid pairs), using a planar (x degree = y degree = 1) fit in x and y .

543 (ii) the *ref_surf/complex_surface_flag* is set to 1.

544 The misfit parameters are reported in the *ref_surf* group: The final chi-squared statistic is
 545 reported as *ref_surf/misfit_chi2r*, equal to the chi-squared statistic divided by the number of
 546 degrees of freedom in the solution; the final RMS of the scaled residuals is reported as
 547 *ref_surf/misfit_rms*.

548 3.3 Reference-shape Correction Error Estimates

549 We first calculate the errors in the corrected surface heights for segments included in the
 550 reference-surface fit. We form a second covariance matrix, \mathbf{C}_1 , whose diagonal elements are the
 551 maximum of the squares of the segment errors and $\langle r^2 \rangle$. We estimate the covariance matrix for
 552 the height estimates:

$$\mathbf{C}_m = \mathbf{G}^{-g} \mathbf{C}_1 \mathbf{G}^{-gT} \quad 9$$

553 The square roots of the diagonal values of \mathbf{C}_m give the estimated errors in the surface-polynomial
 554 and height estimates due to short-spatial-scale errors in the segment heights. If there are N_{coeff}
 555 coefficients in the surface-shape polynomial, and $N_{shape-cycles}$ cycles included in the surface-shape
 556 fit, then the first N_{coeff} diagonal elements of \mathbf{C}_m give the square of the errors in the surface-shape
 557 polynomial and the last $N_{shape-cycles}$ give the errors in the surface heights for the cycles included in
 558 the fit. The portion of \mathbf{C}_m that refers only to the surface shape and surface-shape change
 559 components is $\mathbf{C}_{m,s}$.

560 **3.4 Calculating corrected height values for repeats with no selected pairs**

561 Once the surface polynomial has been established from the edited data set, corrected heights are
 562 calculated for the unselected cycles (*i.e.* those from which all pairs were removed in the editing
 563 steps): For the segments among these cycles, we form a new surface and slope-change design
 564 matrix, $[\mathbf{S}, \mathbf{S}_t]$ and multiply it by $[\mathbf{s}, \mathbf{s}_t]$ to give the surface-shape correction:

$$\mathbf{z}_c = \mathbf{z} - [\mathbf{S}, \mathbf{S}_t][\mathbf{s}, \mathbf{s}_t] \quad 10$$

565 Here, \mathbf{s} is the surface-shape polynomial, and \mathbf{s}_t is the slope-change-rate estimate. This gives up
 566 to fourteen corrected-height values per unselected cycle. From among these, we select the
 567 segment with the minimum error, as calculated in the next step.

568 The height errors for segments from cycles not included in the surface-shape fit are calculated:

$$\sigma_{z,c}^2 = \text{diag}([\mathbf{S}, \mathbf{S}_t]\mathbf{C}_{m,s}[\mathbf{S}, \mathbf{S}_t]^T) + \sigma_z^2 \quad 11$$

569 Here σ_z is the error in the segment height, and $\sigma_{z,c}$ is the error in the corrected height. The
 570 results of these calculations give a height and a height error for each unselected segment. To
 571 obtain a corrected elevation for each repeat that contains no selected pairs, we identify the
 572 segment from that repeat that has the smallest error estimate, and report the value z_c as that
 573 repeat's *ptx/h_corr*, and use $\sigma_{z,c}$ as its error (*ptx/h_corr_sigma*).

574 **3.5 Calculating systematic error estimates**

575 The errors that have been calculated up to this point are due to errors in fitting segments to
 576 photon-counting data and due to inaccuracies in the polynomial fitting model. Additional error
 577 components can result from more systematic errors, such as errors in the position of ICESat-2 as
 578 derived from POD, and pointing errors from PPD. These are estimated in the ATL06
 579 *sigma_geo_xt*, *sigma_geo_at*, and *sigma_geo_r* parameters, and their average for each repeat is
 580 reported in the *cycle_stats* group under the same parameter names. The geolocation component
 581 of the total height is the product of the geolocation error and the surface slope, added in
 582 quadrature with the vertical height error:

$$\sigma_{h,systematic} = \left[\left(\frac{dh}{dx} \sigma_{geo,AT} \right)^2 + \left(\frac{dh}{dy} \sigma_{geo,XT} \right)^2 + \sigma_{geo,r}^2 \right]^{1/2} \quad 12$$

583 For selected segments, which generally come from pairs containing two high-quality height
 584 estimates, dh/dy is estimated from the ATL06 *dh_fit_dy* parameter. For unselected segments, it is
 585 based on the y component of the reference-surface slope, as calculated in section 4.2.

586 The error for a single segment's corrected height is:

$$\sigma_{h,total} = [\sigma_{h,systematic}^2 + \sigma_{h,c}^2]^{1/2} \quad 13$$

587 This represents the total error in the surface height for a single corrected height. In most cases,
 588 error estimates for averages of ice-sheet quantities will depend on errors from many segments
 589 from different reference points, and the spatial scale of the different error components will need
 590 to be taken into account in error propagation models. To allow users to separate these effects,
 591 we report both the uncorrelated error, */ptx/h_corr_sigma*, and the component due only to
 592 systematic errors, */ptx/h_corr_sigma_systematic*. The total error is the quadratic sum of the two,
 593 as described in equation 13.

594 3.6 Calculating shape-corrected heights for crossing-track data

595 Locations where groundtracks cross provide opportunities to check the accuracy of
 596 measurements by comparing surface-height estimates between the groundtracks, and also offers
 597 the opportunity to generate elevation-change time series that have more temporal detail than the
 598 91-day repeat cycle can offer for repeat-track measurements. Because the groundtracks
 599 converge for latitudes close to the 88-degree limit of coverage, the crossover data are not as
 600 useful at the highest latitudes, and are computationally expensive to calculate, we only calculate
 601 values in the group for reference points between 86°S and 86°N.

602 At these crossover points, we use the reference surface calculated in 3.5 to calculate corrected
 603 elevations for the crossing tracks. We refer to the track for which we have calculated the
 604 reference surface as the *datum* track, and the other track as the *crossing* track. To calculate
 605 corrected surface heights for the crossing ICESat-2 orbits, we first select all data from the
 606 crossing orbit within a distance *L_search_XT* of the updated reference point on the datum track.
 607 For most datum reference points, this will yield no crossing data, in which case the calculation
 608 for that datum point terminates. If crossing data are found, we then calculate the coordinates of
 609 these points in the reference point's along-track and across-track coordinates. This calculation
 610 begins by transforming the crossing-track data into local northing and easting coordinates
 611 relative to the datum reference-point location:

$$\delta N_c = \frac{\pi R_e}{180} (lat_c - lat_d) \quad 14$$

$$\delta E_c = \frac{\pi R_e}{180} (lon_c - lon_d) \cos (lat_c)$$

612 Here (lat_d, lon_d) are the coordinates of the adjusted datum reference point, (lat_c, lon_c) are the
 613 coordinates of the points on the crossing track, and R_e is the local radius of the WGS84 ellipsoid.
 614 We then convert the northing and easting coordinates into along-track and across-track
 615 coordinates based on the azimuth ϕ of the datum track:

$$\begin{aligned} x_c &= \delta N_c \cos(\phi) + \delta E_c \sin(\phi) \\ y_c &= \delta N_c \sin(\phi) - \delta E_c \cos(\phi) \end{aligned} \quad 15$$

616 Using these coordinates, we proceed as we did in 3.4 and 3.5: we generate S_k and S_{kt} matrices,
 617 use them to correct the data and to identify the data point with the smallest error for each
 618 crossing cycle. We report the time, error estimate, and corrected height for the minimum-error
 619 datapoint from each cycle, as well as the location, pair, and track number corresponding to the
 620 datum point in the */ptx/crossing_track_data* group. Because the crossing angles between the

621 tracks are oblique at high latitudes, a particular crossing track may appear in a few subsequent
 622 datum points; in these cases, we expect that the error estimates should vary with the distance
 623 between the crossing track and the datum track, so that the point with the minimum error should
 624 correspond to the precise crossing location of the two tracks.

625 To help evaluate the quality of crossing-track data we calculate the *along_track_rss* parameter
 626 for each crossing-track measurement. This parameter gives the RSS of the differences between
 627 each segment's endpoint heights and the heights of the previous and subsequent segments. A
 628 segment that is consistent with the previous and next segments in slope and elevation will have a
 629 small value for this parameter, a segment that is inconsistent (and thus potentially in error) will
 630 have a large value. Crossing-track measurements that have values greater than 10 m are
 631 excluded from ATL11 and do not appear in the dataset.

632 3.7 Calculating parameter averages

633 ATL11 contains a variety of parameters that mirror parameters in ATL06, but are averaged to the
 634 140-m ATL11 resolution. Except where noted otherwise, these quantities are weighted averages
 635 of the corresponding ATL06 values. For selected pairs (i.e. those included in the reference-
 636 surface fit), the parameters are averaged over the selected segments from each cycle, using
 637 weights derived from their formal errors, *h_li_sigma*. The parameter weighted average for the N_k
 638 segments from cycle k is then:

$$\langle q \rangle = \frac{\sum_{i=1}^{N_k} |\sigma_i^{-2}| q_i}{\sum_{i=1}^{N_k} |\sigma_i^{-2}|} \quad 16$$

639 Here q_i are the parameter values for the segments. For repeats with no selected pairs, recall that
 640 the corrected height for only one segment is reported in */ptx/h_corr*; for these, we simply report
 641 the corresponding parameter values for that selected segment.

642

643 3.8 Output data editing

644 The output data product includes cycle height estimates only for those cycles that have
 645 non-systematic error estimates (*/ptx/h_corr_sigma*) less than 15 m. All other heights (and their
 646 errors) are reported as *invalid*.

647

648

649 **4.0 LAND ICE PRODUCTS: LAND ICE H (T)(ATL 11/L3B)**

650 Each ATL11 file contains data for a single reference ground track, for one of the subregions
 651 defined for ATLAS granules (see Figure 6-3). The ATL11 consists of three top-level groups, one
 652 for each beam pair (*pt1*, *pt2*, *pt3*). Within each pair-track group, there are datasets that give the
 653 corrected heights for each cycle, their errors, and the reference-point locations. Subgroups
 654 (*cycle_stats*, and *ref_surf*) provide a set of data-quality parameters, and ancillary data describing
 655 the fitting process, and use the same ordering and coordinates as the top-level group (i.e. any
 656 dataset within the */ptx/cycle_stats* and */ptx/ref_surf* groups refers to the same latitude, longitude,
 657 and reference points as the corresponding measurements in the */ptx/* groups.) The
 658 *crossing_track_data* group gives height measurements at crossover locations, and has its own set
 659 of locations and
 660

661 **4.1.1 File naming convention**

662 ATL11 files are named in the following format:

663 `ATL11_ttttgg_cccc_rrr_vv.h5`

664 Here *tttt* is the rgt number, *gg* is the granule-region number, *cccc* gives the first and last cycles of
 665 along-track data included in the file (e.g. `_0308_` would indicate that cycles three through eight,
 666 inclusive, might be included in the along-track solution), and *rrr* is the release number. and *vv* is
 667 the version number, which is set to one the first time a granule is generated for a given data
 668 release, and is incremented by one if the granule is regenerated.

669

670 **4.2 /ptx group**

671 **4.3**

672 shows the datasets in the *ptx* groups. This group gives the principal output parameters of the
 673 ATL11. The corrected repeat measurements are in */ptx/h_corr*, which gives improved height
 674 measurements based on a surface fit to valid data at paired segments. The associated reference
 675 coordinates, */ptx/latitude* and */ptx/longitude* give the reference point location, with averaged
 676 times per repeat, */ptx/delta_time*. For repeats with no selected pairs, the corrected height is that
 677 from the selected segment with the lowest error. Two error metrics are given in
 678 */ptx/h_corr_sigma* and */ptx/h_corr_sigma_systematic*. The first gives the error component due to
 679 ATL06 range errors and due to uncertainty in the reference surface. The second gives the
 680 component due to geolocation and radial-orbit errors that are correlated at scales larger than one
 681 reference point; adding these values in quadrature gives the total per-cycle error. Values are only
 682 reported for */ptx/h_corr*, */ptx/h_corr_sigma*, and */ptx/h_corr_sigma_systematic* for those cycles
 683 whose uncorrelated errors are less than 15 m; all others are reported as *invalid*. A
 684 */ptx/quality_summary* is included for each cycle, based on fit statistics from ATL06.

685

686

Table 4-1 Parameters in the /ptx/ group

Parameter	Units	Dimensions	Description
<i>cycle_number</i>	counts	$I \times N_{cycles}$	Cycle number for each column of the data
<i>latitude</i>	degrees North	$N_{pts} \times I$	Reference point latitude
<i>longitude</i>	degrees East	$N_{pts} \times I$	Reference point longitude
<i>ref_pt</i>	counts	$N_{pts} \times I$	The reference point number, <i>m</i> , counted from the equator crossing of the RGT.
<i>delta_time</i>	seconds	$N_{pts} \times N_{cycles}$	mean GPS time for the segments for each cycle
<i>h_corr</i>	meters	$N_{pts} \times N_{cycles}$	the mean corrected height
<i>h_corr_sigma</i>	meters	$N_{pts} \times N_{cycles}$	the formal error in the corrected height
<i>h_corr_sigma_systematic</i>	meters	$N_{pts} \times N_{cycles}$	the magnitude of the RSS of all errors that might be correlated at scales larger than a single reference point (e.g. pointing errors, GPS errors, etc)
<i>quality_summary</i>	counts	$N_{pts} \times N_{cycles}$	summary flag: zero indicates high-quality cycles: where $\min(\text{signal_selection_source}) \leq 1$ and $\min(\text{SNR_significance}) < 0.02$, and $\text{ATL06_summary_zero_count} > 0$.

687

688 4.4 /ptx/ref_surf group

689 Table 4-2 describes the /ptx/ref_surf group. This group includes parameters describing the
 690 reference surface fit at each reference point. The polynomial coefficients are given in
 691 /ptx/poly_ref_surf, sorted first by total degree, then by x-component degree. Because the
 692 polynomial degree is chosen separately for each reference point, enough columns are provided in
 693 the /ptx/poly_ref_surf and /ptx/poly_ref_surf_sigma to accommodate all possible components up
 694 to 2rd degree in y and 3th degree in x, and absent values are filled in with zeros. The
 695 correspondence between the columns of the polynomial fields and the exponents of the x and y
 696 terms are given in the /ptx/poly_exponent_x and /ptx/poly_exponent_y fields. The time origin for
 697 the slope change is given in the group attribute /ptx/slope_change_t0.

Table 4-2 Parameters in the /ptx/ref_surf group

Parameter	Units	Dimensions	Description
<i>complex_surface_flag</i>	counts	$N_{pts} \times I$	0 indicates that normal fitting was attempted, 1 indicates that the signal selection algorithm rejected too many repeats, and only a linear fit was attempted
<i>rms_slope_fit</i>	counts	$N_{pts} \times I$	the RMS of the slope of the fit polynomial within 50 m of the reference point
<i>e_slope</i>	counts	$N_{pts} \times I$	the mean East-component slope for the reference surface within 50 m of the reference point
<i>n_slope</i>	counts	$N_{pts} \times I$	the mean North-component slope for the reference surface within 50 m of the reference point
<i>at_slope</i>	Counts	$N_{pts} \times I$	Mean along-track component of the slope of the reference surface within 50 m of the reference point
<i>xt_slope</i>		$N_{pts} \times I$	Mean across-track component of the slope of the reference surface within 50 m of the reference point
<i>deg_x</i>	counts	$N_{pts} \times I$	Maximum degree of non-zero polynomial components in x
<i>deg_y</i>	counts	$N_{pts} \times I$	Maximum degree of non-zero polynomial components in y

<i>poly_exponent_x</i>	counts	1×8	Exponents for the x factors in the surface polynomial
<i>poly_exponent_y</i>	counts	1×8	Exponents for the y factors in the surface polynomial
<i>poly_coeffs</i>	counts	$N_{pts} \times 8$	polynomial coefficients (up to degree 3), for polynomial components scaled by 100 m
<i>poly_ref_coeffs_sigma</i>	counts	$N_{pts} \times 8$	formal errors for the polynomial coefficients
<i>ref_pt_number</i>	counts	$N_{pts} \times 1$	Ref point number, counted from the equator crossing along the RGT.
<i>x_atc</i>	meters	$N_{pts} \times 1$	Along-track coordinate of the reference point, measured along the RGT from its first equator crossing.
<i>y_atc</i>	meters	$N_{pts} \times 1$	Across-track coordinate of the reference point, measured along the RGT from its first equator crossing.
<i>rgt_azimuth</i>	degrees	$N_{pts} \times 1$	Reference track azimuth, in degrees east of local north
<i>slope_change_rate_x</i>	years ⁻¹	$N_{pts} \times 1$	rate of change of the x component of the surface slope
<i>slope_change_rate_y</i>	years ⁻¹	$N_{pts} \times 1$	rate of change of the y component of the surface slope
<i>slope_change_rate_x_sigma</i>	years ⁻¹	$N_{pts} \times 1$	Formal error in the rate of change of the x component of the surface slope
<i>slope_change_rate_y_sigma</i>	years ⁻¹	$N_{pts} \times 1$	Formal error in the rate of change of the y component of the surface slope
<i>misfit_chi2r</i>	meters	$N_{pts} \times 1$	misfit chi square, divided by the number of degrees in the solution
<i>misfit_rms</i>	meters	$N_{pts} \times 1$	RMS misfit for the surface-polynomial fit
<i>fit_quality</i>	counts	$N_{pts} \times 1$	Indicates quality of the fit:

			0: no problem identified 1: One or more polynomial coefficient errors larger than 2 2: One or more components of the surface slope has magnitude larger than 0.2 3: Conditions 1 and 2 both true.
--	--	--	------------------------------------------------------------------------------------------------------------------------------------------------------------------------------------------------------------

698
699

700 The slope of the fit surface is given in the *ref_surf/n_slope* and *ref_surf/e_slope* parameters in
 701 the local north and east directions; the corresponding slopes in the along-track and across-track
 702 directions are given in the *ref_surf/xt_slope* and *ref_surf/yt_slope* parameters. For the along-
 703 track points, the surface slope is calculated by evaluating the correction-surface polynomial for a
 704 10-m spaced grid of points extending ± 50 m in *x* and *y* around the reference point, and
 705 calculating the mean slopes of these points. The calculation is performed in along-track
 706 coordinates and then projected onto the local north and east vectors. The *rms_slope_fit*
 707 derived from the same set of points, and is calculated as the RMS of the standard deviations of
 708 the slopes calculated from adjacent grid points, in *x* and *y*.

709

710 **4.5 /ptx/cycle_stats group**

711 The */ptx/cycle_stats* group gives summary information about the segments present for each
 712 reference point. Most parameters are averaged according to equation 14, but for others (e.g.
 713 */ptx/signal_selection_flag_best*, which is the minimum of the signal selection flags for the cycle)
 714 **Table 4-3** describes how the summary statistics are derived.

715

716 **Table 4-3 Parameters in the /ptx/cycle_stats group**

Parameter	Units	Dimensions	Description
<i>ATL06_summary_zero_count</i>	counts	$N_{pts} \times N_{cycles}$	Number of segments with <i>atl06_quality_summary</i> =0 (0 indicates the best-quality data)
<i>h_rms_misfit</i>	meters	$N_{pts} \times N_{cycles}$	Weighted-average RMS misfit between PE heights and along-track land-ice segment fit
<i>r_eff</i>	counts	$N_{pts} \times N_{cycles}$	Weighted-average effective, uncorrected reflectance for each cycle.

Parameter	Units	Dimensions	Description
<i>tide_ocean</i>	meters	$N_{pts} \times N_{cycles}$	Weighted-average ocean tide for each cycle
<i>dac</i>	meters	$N_{pts} \times N_{cycles}$	Dynamic atmosphere correction (mainly the effect of atmospheric pressure on floating-ice elevation).
<i>cloud_flg_atm</i>	counts	$N_{pts} \times N_{cycles}$	Minimum cloud flag from ATL06: Flag indicates confidence that clouds with $OT^* > 0.2$ are present in the lower 3 km of the atmosphere based on ATL09
<i>cloud_flg_asr</i>	counts	$N_{pts} \times N_{cycles}$	Minimum apparent-surface-reflectance - based cloud flag from ATL06: Flag indicates confidence that clouds with $OT > 0.2$ are present in the lower 3 km of the atmosphere based on ATL09
<i>bsnow_h</i>	meters	$N_{pts} \times N_{cycles}$	Weighted-average blowing snow layer height for each cycle
<i>bsnow_conf</i>	counts	$N_{pts} \times N_{cycles}$	Maximum <i>bsnow_conf</i> flag from ATL06: indicates the greatest (among segments) confidence flag for presence of blowing snow for each cycle
<i>x_atc</i>	meters	$N_{pts} \times N_{cycles}$	weighted average of pair-center RGT y coordinates for each cycle
<i>y_atc</i>	meters	$N_{pts} \times N_{cycles}$	weighted mean of pair-center RGT y coordinates for each cycle
<i>ref_pt</i>		$N_{pts} \times N_{cycles}$	Ref point number, counted from the equator crossing along the RGT.
<i>seg_count</i>	counts	$N_{pts} \times N_{cycles}$	Number of segments marked as valid for each cycle. Equal to 0 for those cycles not included in the reference-surface shape fit.
<i>min_signal_selection_source</i>	counts	$N_{pts} \times N_{cycles}$	Minimum of the ATL06 <i>signal_selection_source</i> value (indicates the highest-quality segment in the cycle)
<i>min_snr_significance</i>	counts	$N_{pts} \times N_{cycles}$	Minimum of <i>SNR_significance</i> (indicates the quality of the best segment in the cycle)

Parameter	Units	Dimensions	Description
<i>sigma_geo_h</i>	meters	$N_{pts} \times N_{cycles}$	Root-mean-weighted-square-average total vertical geolocation error due to PPD and POD
<i>sigma_geo_at</i>	meters	$N_{pts} \times N_{cycles}$	Root-mean-weighted-square-average local-coordinate x horizontal geolocation error for each cycle due to PPD and POD
<i>sigma_geo_xt</i>	meters	$N_{pts} \times N_{cycles}$	Root-mean-weighted-square-average local-coordinate y horizontal geolocation error for each cycle due to PPD and POD
<i>h_mean</i>	meters	$N_{pts} \times N_{cycles}$	Weighted average of surface heights, not including the correction for the reference surface

717 *OT (optical thickness) is a measure of signal attenuation used in atmospheric calculations. This
 718 parameter discussed in ICESat-2 atmospheric products (ATL09)

719

720 **4.6 /ptx/crossing_track_data group**

721 The /ptx/crossing_track_data group (Table 4-4) contains elevation data at crossover locations.
 722 These are locations where two ICESat-2 pair tracks cross, so data are available from both the
 723 datum track, for which the granule was generated, and from the crossing track. The data in this
 724 group represent the elevations and times from the crossing tracks, corrected using the reference
 725 surface from the datum track. Each set of values gives the data from a single segment on the
 726 crossing track, that was selected as having the minimum error among all segments on the
 727 crossing track within the $2 L_{search_XT} - by - 2 L_{search_AT}$ window around the reference point
 728 on the datum track. The systematic errors are evaluated based on the magnitude of the reference-
 729 surface slope and the magnitude of the horizontal geolocation error of the crossing-track data.
 730 Attributes for the group specify the track number and pair-track number of the crossing track.

731

Table 4-4 Parameters in the /ptx/crossing_track_data group

Parameter	Units	Dimensions	Description
<i>ref_pt</i>	counts	$N_{XO} \times 1$	the reference-point number for the datum track
<i>delta_time</i>	years	$N_{XO} \times 1$	time relative to the ICESat-2 reference epoch
<i>h_corr</i>	meters	$N_{XO} \times 1$	WGS-84 height, corrected for the ATL11 surface shape

<i>h_corr_sigma</i>	meters	$N_{XO} \times 1$	error in the height estimate
<i>h_corr_sigma_systematic</i>	meters	$N_{XO} \times 1$	systematic error in the height estimate
<i>ocean_tide</i>	Meters	$N_{XO} \times 1$	Ocean-tide estimate for the crossing track
<i>dac</i>	Meters	$N_{XO} \times 1$	Dynamic atmosphere correction for the crossing track
<i>latitude</i>	degrees	$N_{XO} \times 1$	latitude of the crossover point
<i>longitude</i>	degrees	$N_{XO} \times 1$	longitude of the crossover point
<i>cycle_number</i>	counts	$N_{XO} \times 1$	Cycle number for the crossing data
<i>rgt</i>	counts	$N_{XO} \times 1$	The RGT number for the crossing data
<i>spot_crossing</i>	counts	$N_{XO} \times 1$	The spot number for the crossing data
<i>atl06_quality_summary</i>	counts	$N_{XO} \times 1$	quality flag for the crossing data derived from ATL06. 0 indicates no problems detected, 1 indicates potential problems
<i>along_track_rss</i>	meters	$N_{XO} \times 1$	Root sum of the squared differences between the heights of the endpoints for the crossing-track segment and the centers of the previous and next segments

732

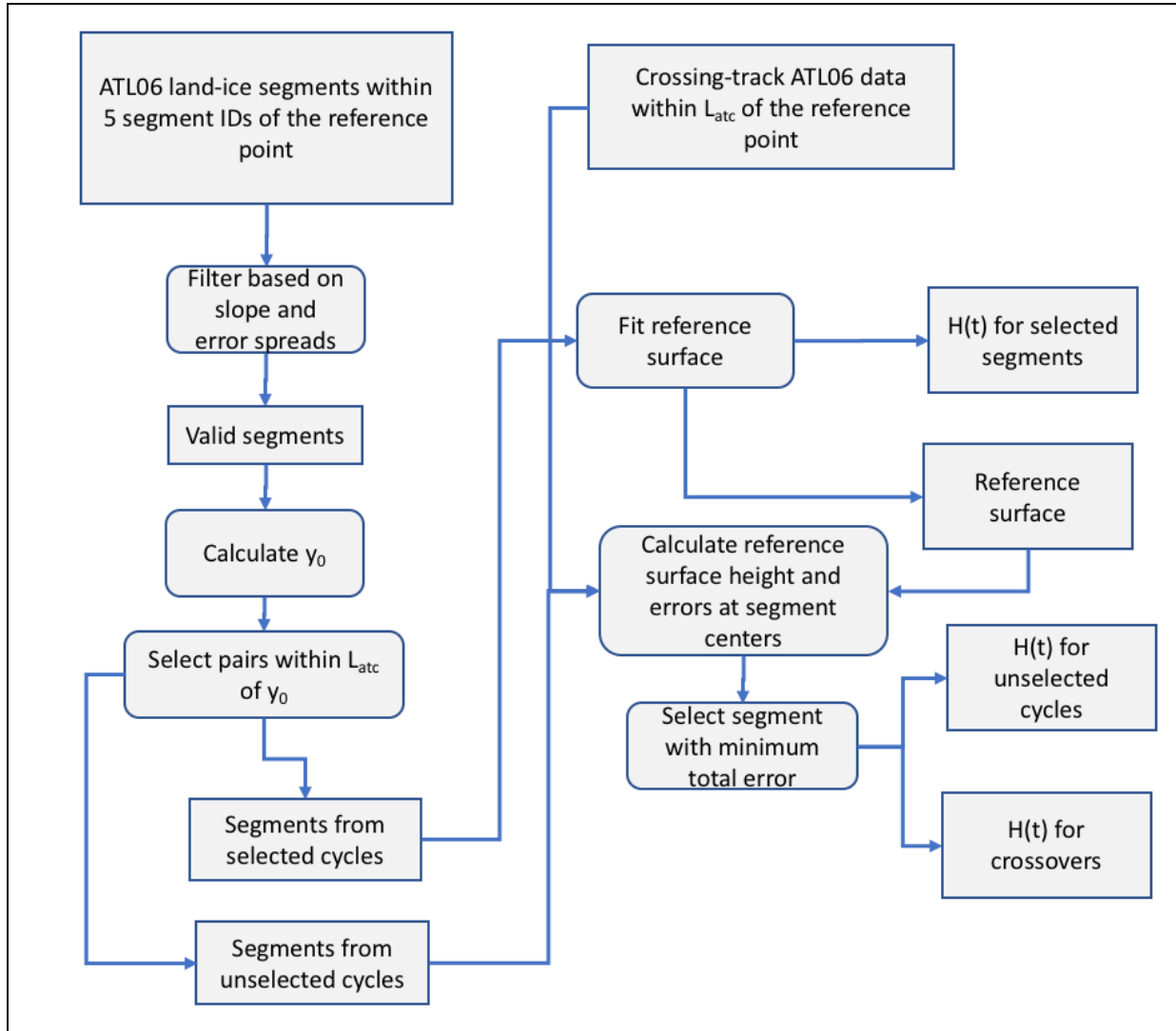
733

734 5.0 ALGORITHM IMPLEMENTATION

735

736

Figure 5-1 Flow Chart for ATL11 Surface-shape Corrections



737

738

739 The following steps are performed for each along-track reference point.

740

741

742

743

744

1. Segments with *segment_id* within $N_search/2$ of the reference-point number, are selected.
2. Valid segments are identified based on estimated errors, the *ATL06_quality_summary* parameter, and the along- and across-track segment slopes. Valid pairs, containing valid measurements from two different beams, are also identified.

- 745 3. The location of the reference point is adjusted to allow the maximum number of repeats
746 with at least one valid pair to fall within the across-track search distance of the reference
747 point.
748 4. The reference surface is fit to pairs with two valid measurements within the search
749 distance of the reference point. This calculation also produces corrected heights for the
750 selected pairs and the errors in the correction polynomial coefficients.
751 5. The correction surface is used to derive corrected heights for segments not selected in
752 steps 1-3, and the height for the segment with the smallest error is selected for each
753 6. The reference surface is used to calculate heights for external (pre-ICESat-2) laser
754 altimetry data sets and crossover ICESat-2 data.

755 A schematic of this calculation is shown in Figure 5-1.

756 5.1.1 Select ATL06 data for the current reference point

757 **Inputs:**

758 *ref_pt*: segment number for the current reference point

759 *track_num*: The track number for current point

760 *pair_num*: The pair number for the current point

761 **Outputs:**

762 *D_ATL06*: ATL06 data structure

763 **Parameters:**

764 *N_search*: number of segments to search, around *ref_pt*, equal to 5.

765 **Algorithm:**

- 766 1. For each along-track point, load all ATL06 data from track *track_num* and pair *pair_num* that
767 have *segment_id* within *N_search* of *ref_pt*: These segments have $ref_pt - N_search$
768 $\leq segment_id \leq ref_pt + N_search$.
769 2. Reject any data that have *y_atc* values more than 500 m distant from the nominal pair-track
770 centers (3200 m for pair 1, 0 m for pair 2, -3200 m for pair 3).

771

772 5.1.2 Select pairs for the reference-surface calculation

773 **Inputs:**

774 *ref_pt*: reference point number for the current fit

775 *x_atc_ctr*: Along-track coordinate of the reference point

776 *D_ATL06*: ATL06 data structure

777 *pair_data*: Structure describing ATL06 pairs, includes mean of strong/weak beam *y_atc* and
778 *dh_fit_dy*

779 **Outputs:**

780 **validity flags for each segment:**

781 *valid_segs.x_slope*: Segments identified as valid based on x-slope consistency

782 *valid_segs.data*: Segments identified as valid based on ATL06 parameter values.

783 **Validity flags for each pair:**

784 *valid_pairs*: Pairs selected for the reference-surface calculation

785 *valid_pairs.y_slope*: Pairs identified as valid based on y-slope consistency

786 *y_polyfit_ctr*: y center of the slope regression

787 *ref_surf/complex_surface_flag*: Flag indicating 0: non-complex surface, 1: complex surface.

788

789 **Parameters:**

790 *L_search_XT*: The across-track search distance.

791 *N_search*: Along-track segment search distance

792 *seg_sigma_threshold_min*: Minimum threshold for accepting errors in segment heights, equal to
793 0.05 m.

794 **Algorithm:**

795 1. Flag valid segments based on ATL06 values.

796 1a. Count the cycles that contain at least one pair that has *atl06_quality_flag*=0
797 for both segments. If this number is greater than $N_cycles/3$, set
798 *ref_surf/complex_surface_flag*=0 and set *valid_segs.data* to 1 for segments with
799 *ATL06_quality_summary* equal to 0. Otherwise, set *ref_surf/complex_surface_flag*=1 and set
800 *valid_segs.data* to 1 for segments with *snr_significance* < 0.02.

801 1b. Define *seg_sigma_threshold* as the maximum of 0.05 or three times the median of
802 *sigma_h_li* for segments with *valid_segs.data* equal to 1. Set *valid_segs.data* to 1 for segments
803 with *h_sigma_li* less than this threshold and *ATL06_quality_summary* equal to 0.

804 1c. Define *valid_pairs.data*: For each pair of segments, set *valid_pairs.data* to 1 when
805 both segments are marked as valid in *valid_segs.data*.

806 2. Calculate representative values for the *x* and *y* coordinate for each pair, and filter by distance.

807 2a. For each pair containing two defined values, set *pair_data.x* to the segments' *x_atc*
808 value, and *pair_data.y* to the mean of the segments' *y_atc* values.

809 2b. Calculate *y_polyfit_ctr*, equal to the median of *pair_data.y* for pairs marked valid in
810 *valid_pairs.data*.

811 2c. Set *valid_pairs.ysearch* to 1 for pairs with $|pair_data.y - y_polyfit_ctr| <$
812 *L_search_XT*.

- 813 3. Select pairs based on across-track slope consistency
- 814 3a. Define *pairs_valid_for_y_fit*, for the across-track slope regression if they are marked
815 as valid in *valid_pairs.data*, and *valid_pairs.ysearch*, not otherwise.
- 816 3b. Choose the degree of the regression for across-track slope
- 817 -If the valid pairs contain at least two different *x_atc* values (separated by at least
818 18 m), set the along-track degree, *my_regression_y_degree*, to 1, 0 otherwise.
- 819 -If valid pairs contain at least two different *ref_surf/y_atc* values (separated by at
820 least 18 m), set the across-track degree, *my_regression_y_degree*, to 1, 0 otherwise.
- 821 3c. Calculate the formal error in the y slope estimates: *y_slope_sigma* is the RSS of the
822 *h_li_sigma* values for the two beams in the pair divided by the difference in their *y_atc*
823 values. Based on these, calculate *my_regression_tol*, equal to the maximum of 0.01 or three
824 times the median of *y_slope_sigma* for valid pairs (*pairs_valid_for_y_fit*).
- 825 3d. Calculate the regression of *dh_fit_dy* against *pair_data.x* and *pair_data.y* for valid
826 pairs (*pairs_valid_for_y_fit*). The result is *y_slope_model*, which gives the variation of *dh_fit_dy*
827 as a function of *x_atc* and *y_atc*. Calculate *y_slope_resid*, the residuals between the *dh_fit_dy*
828 values and *y_slope_model* for all pairs in *pair_data*.
- 829 3e. Calculate *y_slope_threshold*, equal to the maximum of *my_regression_tol* and three
830 times the RDE of *y_slope_resid* for valid pairs.
- 831 3f. Mark all pairs with $|y_slope_resid| > y_slope_threshold$ as invalid. Re-establish
832 *pairs_valid_for_y_fit* (based on *valid_pairs.data*, *valid_pairs.y_slope* and *valid_pairs.ysearch*).
833 Return to step 3d (allow two iterations total).
- 834 3g. After the second repetition of 3d-f, use the model to mark all pairs with
835 $|y_slope_resid|$ less than *y_slope_threshold* with 1 in *valid_pairs.y_slope*, 0 otherwise.
- 836 4. Select segments based on along-track slope consistency for both segments in the pair
- 837 4a. Define *pairs_valid_for_x_fit*, valid segments for the along-track slope regression:
838 segments are valid if they come from pairs marked as valid in *valid_pairs.data* and
839 *valid_pairs.ysearch*, not otherwise.
- 840 4b. Choose the degree of the regression for along-track slope
- 841 -If valid segments contain at least two different *x_atc* values set the along-track
842 degree, *mx_regression_x_degree*, to 1, 0 otherwise.
- 843 -If valid segments contain at least two different *y_atc* values, set the across-track
844 degree, *mx_regression_y_degree*, to 1, 0 otherwise.
- 845 4c. Calculate along-track slope regression tolerance, *mx_regression_tol*, equal to the
846 maximum of either 0.01 or three times the median of the *dh_fit_dx_sigma* values for the valid
847 pairs.
- 848 4d. Calculate the regression of *dh_fit_dx* against *pair_data.x* and *pair_data.y* for valid
849 segments (*pairs_valid_for_x_fit*). The result is *x_slope_model*, which gives the variation of

850 dh_fit_dx as a function of $pair_data.x$ and $pair_data.y$. Calculate x_slope_resid , the residuals
 851 between the dh_fit_dx and x_slope_resid for all segments for this reference point, seg_x_center
 852 and $y_polyfit_ctr$.

853 4e. Calculate $x_slope_threshold$, equal to the maximum of either $mx_regression_tol$ or
 854 three times the RDE of x_slope_resid for valid segments.

855 4f. Mark $valid_segs.x_slope$ with $|x_slope_resid| > x_slope_threshold$ as invalid. Re-
 856 establish $valid_pairs.x_slope$ when both $valid_segs.x_slope$ equal 1. Re-establish
 857 $pairs_valid_for_x_fit$. Return to step 4d (allow two iterations total).

858 4g. After the second repetition of 4d-f, mark all segments with $|x_slope_resid|$ less than
 859 $x_slope_threshold$ with 1 in seg_valid_xslope , 0 otherwise. Define $valid_pairs.x_slope$ as 1 for
 860 pairs that contain two segments with $valid_segs.x_slope=1$, 0 otherwise.

861 5. Re-establish $valid_pairs.all$. Set equal to 1 if $valid_pairs.x_slope$, $valid_pairs.y_slope$,
 862 and $valid_pairs.data$ are all valid.

863 5a. Identify $unselected_cycle_segs$, as those $D6.cycles$ where $valid_pairs.all$ are False.

864

865 **5.1.3 Adjust the reference-point y location to include the maximum number of** 866 **cycles**

867 **Inputs:**

868 D_ATL06 : ATL06 structure for the current reference point.

869 $valid_pairs$: Pairs selected based on parameter values and along- and across-track slopes.

870 **Outputs:**

871 ref_surf/y_atc : Adjusted fit-point center y .

872 $valid_pairs$: validity masks for pairs, updated to include those identified as valid based on the
 873 spatial search around y_atc_ctr .

874 **Parameters:**

875 L_search_XT : Across-track search length (equal to 110 m)

876 **Algorithm:**

877 1. Define $y0$ as the mean of the minimum and maximum y_atc for $valid_pairs.all$. Set a
 878 range of y values, $y0_shifts$, as $round(y0) +/- 100$ meters in 2-meter increments.

879 2. For each value of $y0_shifts$ ($y0_shift$), set a counter, $selected_seg_cycle_count$, to the
 880 number of distinct cycles for which both segments of the pair are contained entirely within the y
 881 interval $[y0_shift - L_search_XT, y0_shift + L_search_XT]$. Add to this, the number of distinct
 882 cycles represented by unpaired segments contained within that interval, weighted by 0.01. The
 883 sum is called $score$.

884 3. Search for an optimal y-center value (with the most distinct cycles). Set y_{best} to the
 885 value of $y0_shift$ that maximizes $score$. If there are multiple $y0_shift$ values with the same,
 886 maximum $score$, set to the median of the $y0_shift$ values with the maximum $score$.

887 4. Update $valid_pairs$ to include all pairs with y_atc within +/- L_search_XT from
 888 y_atc_ctr .

889 **5.1.4 Calculate the reference surface and corrected heights for selected pairs**

890 **Inputs:**

891 D_ATL06 : ATL06 structure for the current reference point, containing parameters for each
 892 segment:

893 x_atc : along-track coordinate

894 y_atc : across-track coordinate

895 $delta_t$: time for the segment

896 $pair_data$: Structure containing information about ATL06 pairs. Must include:

897 y_atc : Pair-center across-track coordinates

898 $valid_pairs$: Pairs selected based on parameter values and along- and across-track slope.

899 x_atc_ctr : The reference point along-track x coordinate (equal to ref_surf/x_atc).

900 y_atc_ctr : The reference point along-track x coordinate (equal to ref_surf/y_atc)

901 **Outputs:**

902 ref_surf/deg_x : Degree of the reference-surface polynomial in the along-track direction

903 ref_surf/deg_y : Degree of the reference-surface polynomial in the across-track direction

904 $ref_surf/poly_coeffs$: Polynomial coefficients of the reference-surface fit

905 $ref_surf/poly_coeffs_sigma$: Formal error in polynomial coefficients of the reference-surface fit

906 $ref_surf/slope_change_rate_x$: Rate of change of the x component of the surface slope

907 $ref_surf/slope_change_rate_x_sigma$: Formal error in the rate of change of the x component of
 908 the surface slope

909 $ref_surf/slope_change_rate_y$: Rate of change of the y component of the surface slope

910 $ref_surf/slope_change_rate_y_sigma$: Formal error in the rate of change of the y component of
 911 the surface slope

912 r_seg : Segment residuals from the reference-surface model

913 $/ptx/h_corr$: Partially filled-in per-cycle corrected height for cycles used in reference surface

914 $/ptx/h_corr_sigma$: Partially filled-in per-cycle formal error in corrected height for cycles used in
 915 reference surface

916 ref_surf_cycles : A list of cycles used in defining the reference surface

917 *C_m_surf*: Covariance matrix for the reference-polynomial and surface-change model

918 *fit_columns_surf*: Mask identifying which components of the combined reference-polynomial
 919 and surface-change model were included in the fit.

920 *degree_list_x*: The x degrees corresponding to the columns of matrix used in fitting the reference
 921 surface to the data

922 *degree_list_y*: The y degrees corresponding to the columns of matrix used in fitting the reference
 923 surface to the data

924 *selected_segments*: A set of flags indicating which segments were selected by the iterative
 925 fitting process.

926 Partially filled-n per-cycle ATL11 output variables (see table 4-3) for cycles used in reference
 927 surface

928 **Parameters:**

929 *poly_max_degree_AT*: Maximum polynomial degree for the along-track fit, equal to 3.

930 *poly_max_degree_XT*: Maximum polynomial degree for the across-track fit, equal to 2.

931 *slope_change_t0*: Half the duration of the mission (equal to the time of the last-possible
 932 elevation value minus the time of the start of data collection, divided by two).

933 *max_fit_iterations*: Maximum number of iterations for surface fitting, with acceptable residuals,
 934 equal to 20.

935 *xy_scale*: The horizontal scaling value used in polynomial fits, equal to 100 m

936 *t_scale*: The time scale used in polynomial fits, equal to seconds in 1 year.

937 **Algorithm:**

938 1. Build the cycle design matrix: **G_zp** is a matrix that has one column for each distinct
 939 cycle in *selected_pairs* and one row for each segment whose pair is in *selected_pairs*. For each
 940 segment, the corresponding row of **G_zp** is 1 for the column matching the cycle for that segment
 941 and zero otherwise.

942 2. Select the polynomial degree.

943 The degree of the x polynomial, *ref_surf/deg_x*, is:
 944 $\min(\text{poly_max_degree_AT}, \text{maximum}(\text{number of distinct values of } \text{round}((x_atc - x_atc_ctr)/20)$
 945 among the selected segments in any one cycle) - 1), and the degree of the y polynomial,
 946 *ref_surf/deg_y*, is : $\min(\text{poly_max_degree_XT}, \text{number of distinct values of}$
 947 $\text{round}((\text{pair_data.y_atc} - \text{y_atc_ctr})/20)$ among the selected pairs)

948 3. Perform an iterative fit for the reference-surface polynomial.

949 3a. Define *degree_list_x* and *degree_list_y*: This array defines the x and y degree of the
 950 polynomial coefficients in the polynomial surface model. There is one component for each
 951 unique degree combination of x degrees between 0 and *ref_surf/deg_x* and for y degree between
 952 0 and *ref_surf/deg_y* such that $x_degree + y_degree \leq \max(\text{ref_surf/deg_x}, \text{ref_surf/deg_y})$,

953 except that there is no $x_degree=0$ and $y_degree=0$ combination. They are sorted first by the
 954 sum of the x and y degrees, then by x degree, then by y degree.

955 3b. Define the polynomial fit matrix. **S_fit_poly** has one column for each element of
 956 the polynomial degree arrays, with values equal to $((x_atc - x_atc_ctr)/xy_scale)^{x_degree} ((y_atc -$
 957 $y_atc_ctr)/xy_scale)^{y_degree}$. There is one row in the matrix for every segment marked as *selected*.

958 3c. If the time span is longer than 1.5 years, define slope-change matrices,
 959 **S_fit_slope_change**. The first column of the matrix gives the rate of slope change in the x
 960 component, equal to $(x_atc - x_atc_ctr)/xy_scale * (\delta_time - slope_change_t0)/t_scale$. The
 961 second column gives the rate of slope change in the y component, equal to $(y_atc -$
 962 $y_atc_ctr)/xy_scale * (\delta_time - slope_change_t0)/t_scale$.

963 3d. Build the surface matrix, **G_surf**, and the combined surface and cycle-height matrix,
 964 **G_surf_zp**: The surface matrix is equal to the horizontal catenation of **S_fit_poly**, and, if
 965 defined, **S_fit_slope_change**. The combined surface and cycle-height matrix, **G_surf_zp**, is
 966 equal to the horizontal catenation of **G_surf** and **G_zp**.

967 3e. Subset the fitting matrix. Subset **G_surf_zp** by row to include only rows
 968 corresponding to selected segments to produce **G** (on the first iteration, all are *selected*). Next,
 969 subset **G** by column, first to eliminate all-zero columns, and second to include only columns that
 970 are linearly independent from one another: calculate the normalized correlation between each
 971 pair of columns in **G**, and if the correlation is equal to unity, eliminate the column with the
 972 higher weighted degree ($poly_wt_sum = x_degree + 1.1 * y_degree$, with the factor of 1.1
 973 chosen to avoid ties). Identify the selected columns in the matrix as *fit_columns*. If more than
 974 three of the original surface-change columns have been eliminated, set the
 975 *ref_surf/complex_surface_flag* to *True*, mark all columns corresponding to polynomial
 976 coefficients of combined x and y degree greater than 1 as *False* in *fit_columns*.

977 3f. Check whether the inverse problem is under- or even-determined: If the number of
 978 *selected_segments* is less than the number of columns of **G**, eliminate remaining columns of **G** in
 979 descending order of *poly_wt_sum* until the number of columns of **G** is less than the number of
 980 *selected_segments*.

981 3g. Generate the data-covariance matrix, **C_d**. The data-covariance matrix is a square
 982 matrix whose diagonal elements are the squares of the *h_li_sigma* values for the selected
 983 segments.

984 3h. Calculate the polynomial fit. Initialize **m_surf_zp**, the reference model, to a vector of
 985 zero values, with one value for each column of **G_surf_zp**. Calculate the generalized inverse
 986 (equation 7), of **G**, **G_g**. If the inversion calculation returns an error, or if any row of **G_g** is all-
 987 zero (indicating some parameters are not linearly independent), report fit failure and return.
 988 Otherwise, multiply **G_g** by the subset of *h_li* corresponding to the selected segment to give **m**,
 989 containing values for the parameters selected in *fit_columns*. Fill in the components of
 990 **m_surf_zp** flagged in *fit_columns* with the values in **m**.

991 3i. Calculate model residuals for all segments, *r_seg*, equal to $h_li - G_surf_dz *$
 992 **m_surf_zp**. The subset of *r_seg* corresponding to *selected* segments is *r_fit*.

993 3j. Calculate the fitting tolerance, r_tol , equal to three times the RDE of the
 994 r_fit/h_li_sigma for all *selected* segments. Calculate the reduced chi-squared value for these
 995 residuals, $ref_surf/misfit_chi2$, equal to $r_fit^T C_d^{-1} r_fit$. Calculate the P value for the misfit,
 996 equal to one minus the CDF of a chi-squared distribution with $m-n$ degrees of freedom for
 997 $ref_surf/misfit_chi2$, where m is the number of rows in \mathbf{G} , and n is the number of columns.

998 3k. If the P value is less than 0.025 and fewer than $max_fit_iterations$ have taken place,
 999 mark all segments for which $|r_seg/h_li_sigma| < r_tol$ as *selected*, and return to 3e. Otherwise,
 1000 continue to 3k.

1001 3l. Propagate the errors. Based on the most recent value of $\mathbf{C_d}$, generate a revised data-
 1002 covariance matrix, $\mathbf{C_dp}$, whose diagonal values are the maximum of h_li_sigma and
 1003 $RDE(r_fit)$. Calculate the model covariance matrix, $\mathbf{C_m}$ using equation 9. If any of the
 1004 diagonal elements of $\mathbf{C_m}$ are larger than 10^4 , report a fit failure and return. Fill in elements of
 1005 $\mathbf{m_surf_zp}$ that are marked as valid in $fit_columns$ with the square roots of the corresponding
 1006 diagonal elements of $\mathbf{C_m}$. If any of the errors in the polynomial coefficients are larger than 2,
 1007 set $ref_surf/fit_quality=1$.

1008 4. Return a list of cycles used in determining the reference surface in ref_surf_cycles . These
 1009 cycles have columns in \mathbf{G} that contain a valid pair, and for which the steps 3e and 3j did not
 1010 eliminate the degree of freedom. For these cycles, partially fill in the values of $/ptx/h_corr$ and
 1011 $/ptx/h_corr_sigma$, from \mathbf{m} and $\mathbf{m_sigma}$. Similarly, fill in values for
 1012 $/ptx/h_corr_sigma_systematic$ (Equation 12) and $/ptx/delta_time$, as well as all variables in Table
 1013 4-3. Set $/ptx/h_corr$, $/ptx/h_corr_sigma$, $/ptx/h_corr_sigma_systematic$ to NaN for those cycles
 1014 that have uncorrelated error estimates greater than 15 m.

1015 Values from Table 4-2 defining the fitted reference surface are also reported including
 1016 $ref_surf/poly_coeffs$, and $ref_surf/poly_coeffs_sigma$, $ref_surf/slope_change_rate_x$,
 1017 $ref_surf/slope_change_rate_y$, $ref_surf/slope_change_rate_x_sigma$, and
 1018 $ref_surf/slope_change_rate_y_sigma$.

1019 Return $\mathbf{C_m_surf}$, the portion of $\mathbf{C_m}$ corresponding to the polynomial and slope-change
 1020 components of $\mathbf{C_m}$. Return $selected_cols_surf$, the subset of $selected_cols$ corresponding to the
 1021 surface polynomial and slope-change parameters.

1022 Return the reduced chi-square value for the last iteration, $ref_surf/misfit_chi2r$, equal to
 1023 $ref_surf/misfit_chi2/(m-n)$.

1024

1025 5.1.5 Calculate corrected heights for cycles with no selected pairs.

1026 **Inputs:**

1027 $\mathbf{C_m_surf}$: Covariance matrix for the reference-surface model.

1028 $degree_list_x$, $degree_list_y$: List of x-, y-, degrees for which the reference-surface calculation
 1029 attempted an estimate.

1030 *selected_cols_surf*: Parameters of the combined reference-surface and slope-change model for
 1031 which the inversion returned a value. There should be one value for each row/column of
 1032 **C_m_surf**.

1033 *x_atc_ctr, y_atc_ctr*: Center point for the surface fit (equal to *ref_surf/x_atc, ref_surf/y_atc*)

1034 *selected_segments*: Boolean array indicating segments selected for the reference-surface
 1035 calculation

1036 *valid_segs.x_slope*: Segments identified as valid based on x-slope consistency

1037 *valid_segs.data*: Segments identified as valid based on ATL06 parameter values.

1038 *pair_number*: Pair number for each segment

1039 *h_li*: Land-ice height for each segment

1040 *h_li_sigma*: Formal error in *h_li*.

1041 */ptx/h_corr*: Partially filled-in per-cycle corrected height

1042 */ptx/h_corr_sigma*: Partially filled-in per-cycle corrected height error

1043 *ref_surf/poly_coefs*: Polynomial coefficients from 2-d reference-surface fit

1044 *ref_surf_cycles*: A list of cycles used in defining the reference surface

1045 *ref_surf/slope_change_rate_x, ref_surf/slope_change_rate_y*: Rate of change of the x and y
 1046 components of the surface slope

1047 *ref_surf/N_slope, ref_surf/E_slope*: slope components of reference surface

1048 *sigma_geo_r*: Radial component of the geolocation error for the crossing track

1049 *D_ATL06*: ATL06 data structure

1050 Partially filled-in per-cycle ATL11 output variables (see table 4-3)

1051 **Outputs:**

1052 */ptx/h_corr*: Per-cycle corrected height

1053 */ptx/h_corr_sigma*: Per-cycle corrected height error

1054 *selected_segments*: A set of arrays listing the selected segments for each cycle.

1055 Per-cycle ATL11 output variables (see table 4-3).

1056 **Algorithm:**

1057 1. Identify the segments marked as valid in *valid_segs.data* and *valid_segs.x_slope* that are not
 1058 members of the cycles in *ref_surf_cycles*. Label these as *non_ref_segments*.

1059 2. Build **G_other**, a polynomial-fitting matrix for the *non_ref_segments*. **G_other** will include
 1060 only the polynomial components listed in *degree_list_x* and *degree_list_y*, and (if the mission
 1061 has been going on for at least 1.5 years) the slope-change components. Multiply **G_other** by
 1062 [*ref_surf/poly_coefs, ref_surf/slope_change_rate_x, ref_surf/slope_change_rate_y*] to give
 1063 corrected heights, *z_kc*.

1064 3. Take the subset of **G_other** corresponding to the components in *fit_cols_surf* to make
 1065 **G_other_surf**. Propagate the polynomial surface errors and surface-height errors for
 1066 *non_ref_segments* based on **G_other_surf**, **C_m_surf**, and *h_li_sigma* using equation
 1067 11. These errors are *z_kc_sigma*.

1068 4. Identify the segments in *non_ref_segments* for each cycle, and, from among these, select the
 1069 one with the smallest *z_kc_sigma*. If, for this cycle, *z_kc_sigma* is less than 15 m, fill in the
 1070 corresponding values of */ptx/h_corr* and */ptx/h_corr_sigma*. For cycles containing no valid
 1071 segments, report invalid data as NaN. Similarly, fill in the variables in Table 4-3, with the value
 1072 from the segment with the smallest *z_kc_sigma*.

1073

1074 **5.1.6 Calculate corrected heights for crossover data points**

1075 **Inputs:**

1076 *C_m_surf*: Covariance matrix for the reference surface model.

1077 *C_m_surf*: Covariance matrix for the reference-surface model.

1078 *x_atc_ctr, y_atc_ctr*: Center point for the surface fit, in along-track coordinates

1079 *lat_d, lon_d*: Latitude and longitude for the adjusted datum reference point (from */ptx/latitude,*
 1080 */ptx/longitude*)

1081 *PT*: Pair track for the surface fit

1082 *RGT*: RGT for the surface fit

1083 *ref_surf/rgt_azimuth*: The azimuth of the RGT, relative to local north

1084 *lat_c, lon_c*: Location for crossover data

1085 *time_c*: Time for crossover data

1086 *h_c*: Elevations for crossover data

1087 *sigma_h_c*: Estimated errors for crossover data

1088 **Outputs:**

1089 *ref_pt*: reference point (not for the crossing track) (ben, which one then?)

1090 *pt*: pair track for the crossing-track points

1091 *crossing_track_data/rgt*: Reference ground track for the crossing-track point

1092 *crossing_track_data/delta_time*: time for the crossing-track point

1093 *crossing_track_data/h_corr*: corrected elevation for the crossing-track points

1094 *crossing_track_data/h_corr_sigma*: error in the corrected elevation for the crossing_track points

1095 *crossing_track_data/h_corr_sigma_systematic*: Error component in the corrected elevation due
 1096 to pointing and orbital errors.

1097 *crossing_track_data/along_track_rss:*

1098 **Parameters:**

1099 *L_search_XT:* Across-track search distance

1100 **Algorithm (executed independently for the data from each cycle of the mission):**

1101 1. Project data points into the along-track coordinate system:

1102 1a: Calculate along-track and across-track vectors:

1103 $x_hat = [\cos(\text{ref_surf}/\text{rgt_azimuth}), \sin(\text{ref_surf}/\text{rgt_azimuth})]$

1104 $y_hat = [\sin(\text{ref_surf}/\text{rgt_azimuth}), -\cos(\text{ref_surf}/\text{rgt_azimuth})]$

1105 1b. Calculate the R_earth , the WGS84 radius at lat_d .

1106 1c: Project the crossover data points into a local projection centered on the fit
1107 center:

1108 $N_d = R_earth (\text{lat_c} - \text{lat_d})$

1109 $E_d = R_earth \cos(\text{lat_d}) (\text{lon_c} - \text{lon_d})$

1110 1d: Calculate the x and y coordinates for the data points, relative to the fit-center point:

1111 $dx_c = \langle x_hat, [E_c, N_c] \rangle$

1112 $dy_c = \langle y_hat, [E_c, N_c] \rangle$

1113 Here $\langle \mathbf{a}, \mathbf{b} \rangle$ is the inner (dot) product of \mathbf{a} and \mathbf{b} .

1114 2. Calculate the fitting matrix using equation 6.

1115 3. Calculate the errors at each point using the fitting matrix and C_m , using on equation 11.

1116 4. Select the minimum-error data point and report the values in **Error! Reference source not**
1117 **found..**

1118 5. Calculate the systematic error in the corrected height:

1119 $\text{crossing_track_data}/h_sigma_sigma_systematic = (\text{sigma_geo_r}^2 + (N_d$
1120 $\text{ref_surf}/n_slope)^2 + ((E_d \text{ref_surf}/e_slope)^2)^{1/2}$

1121 6. Calculate the along-track RSS for the selected segment. For each selected crossing segment
1122 calculate the endpoint heights (equal to the segment center height plus or minus 20 meters times
1123 the segment's along-track slope) and calculate the RSS of the differences between these heights
1124 and the center heights of the previous and subsequent segments. If this RSS difference is greater
1125 than 10 m for any cycle, do not report any parameters for that segment's cycle.

1126 **5.1.7 Provide error-averaged values for selected ATL06 parameters**

1127 **Inputs:**

1128 *ATL06 data structure:* ATL06 data to be averaged

1129 *Selected_segments:* A set of arrays listing the selected segments for each cycle.

1130 *Parameter_list*: A list of parameters to be averaged

1131 **Outputs:**

1132 *Parameter_averages*: One value for each parameter and each cycle

1133 **Algorithm:**

1134 1. For each cycle, select the values of *h_li_sigma* based on the values within *selected_segments*.
1135 Calculate a set of weights, w_i , such that the sum of the weights is equal to 1 and each weight is
1136 proportional to the inverse square of *h_li_sigma*. If only one value is present in
1137 *selected_segments*, $w_1=1$.

1138 2. For each parameter, multiply the weights for each cycle by the parameter values, report the
1139 averaged value in *parameter_averages*.

1140 **5.1.8 Provide miscellaneous ATL06 parameters**

1141 **Inputs:**

1142 *ATL06 data structure*: ATL06 data to be averaged

1143 *Selected_segments*: A set of arrays listing the selected segments for each cycle.

1144 **Outputs:**

1145 Weighted-averaged parameter values, with one value per cycle, filled in with NaN for cycles
1146 with no selected segments

1147 *cycle_stats/h_robust_sprd*

1148 *h_li_rms_mean* (*ben*, I don't see this in the list)

1149 *cycle_stats/r_eff*

1150 *cycle_stats/tide_ocean*

1151 *cycle_stats/dac*

1152 *cycle_stats/bsnow_h*

1153 *cycle_stats/x_atc*

1154 *cycle_stats/y_atc*

1155 *cycle_stats/sigma_geo_h*

1156 *cycle_stats/sigma_geo_at*

1157 *cycle_stats/sigma_geo_xt*

1158 *cycle_stats/h_mean*

1159 Parameter minimum values, with one value per cycle, filled in NaN for cycles with no selected
1160 segments:

1161 *cycle_stats/cloud_flg_asr*

1162 *cycle_stats/cloud_flg_atm*

1163 *cycle_stats/bsnow_conf*

1164 Other parameters:

1165 *cycle_stats/strong_spot*: The laser beam number for the strong beam in the pair

1166 **Algorithm:**

1167 1. Select the segments for the cycle indicated in *selected_segments* from the
1168 *ATL06_data_structure*.

1169 2: Based on *h_li_sigma*, calculate the segment weights using equation 14.

1170 3. For ATL06 parameters *h_robust_sprd*, *h_li_rms*, *r_eff*, *tide_ocean*, *dac*, *bsnow_h*, *x_atc*,
1171 *y_atc*, *sigma_geo_h*, *sigma_geo_at*, *sigma_geo_xt*, and *h_mean* calculate the weighted average
1172 of the parameter based on the segment weights. The output parameter names are the same as the
1173 input parameter names in the *cycle_stats* group.

1174 4. For ATL06 parameters *cloud_flg_asr* and *cloud_flg_atm* report the best (minimum) value
1175 from among the selected values. For *bsnow_conf* report the maximum value from among the
1176 selected values.

1177 5. For the *cycle_stats/strong_spot* attribute, report the laser beam number for the strong beam in
1178 the pair.

1179

1180 **5.1.9 Characterize the reference surface**

1181 **Inputs:**

1182 *poly_coeffs*: Coefficients of the surface polynomial

1183 *rgt_azimuth*: the azimuth of the reference ground track

1184 **Outputs:**

1185 *ref_surf/n_slope*: the north component of the reference-surface slope

1186 *ref_surf/e_slope*: the east component of the reference-surface slope

1187 *ref_surf/at_slope*: the along-track component of the reference-surface slope

1188 *ref_surf/xt_slope*: the across-track component of the reference-surface slope

1189 *ref_surf/rms_slope_fit*: the rms slope of the reference surface

1190 **Procedure:**

- 1191 1. Calculate the coordinates of a grid of northing and easting offsets around the reference points,
1192 each between -50 m and 50 m in 10-meter increments: dN , dE
- 1193 2. Translate the coordinates into along and across-track coordinates:
- 1194 $dx = \cos(\text{rgt_azimuth}) * dN + \sin(\text{rgt_azimuth}) * dE$
- 1195 $dy = \sin(\text{rgt_azimuth}) * dN - \cos(\text{rgt_azimuth}) * dE$
- 1196 3. Calculate the polynomial surface elevations for the grid points by evaluating the polynomial
1197 surface at dx and dy : z_poly
- 1198 4. Fit a plane to z_poly as a function of dN and dE . The North coefficient of the plane is
1199 ref_surf/n_slope , the east component is ref_surf/e_slope , the RMS misfit of the plane is
1200 ref_surf/rms_slope_fit . If either component of the slope has a magnitude larger than 0.2, add 2 to
1201 $ref_surf/fit_quality$.
- 1202 5. Fit a plane to z_poly as a function of dx and dy . The along-track coefficient of the plane is
1203 ref_surf/at_slope , the across-track component is ref_surf/xt_slope .
- 1204

1205 **6.0 APPENDIX A: GLOSSARY**

1206 This appendix defines terms that are used in ATLAS ATBDs, as derived from a document
1207 circulated to the SDT, written by Tom Neumann. Some naming conventions are borrowed from
1208 **Spots, Channels and Redundancy Assignments** (ICESat-2-ATSYS-TN-0910) by P. Luers.
1209 Some conventions are different than those used by the ATLAS team for the purposes of making
1210 the data processing and interpretation simpler.

1211

1212 **Spots.** The ATLAS instrument creates six spots on the ground, three that are weak and three that
1213 are strong, where strong is defined as approximately four times brighter than weak. These
1214 designations apply to both the laser-illuminated spots and the instrument fields of view. The
1215 spots are numbered as shown in Figure 1. At times, the weak spots are leading (when the
1216 direction of travel is in the ATLAS +x direction) and at times the strong spots are leading.
1217 However, the spot number does not change based on the orientation of ATLAS. The spots are
1218 always numbered with 1L on the far left and 3R on the far right of the pattern. Not: beams,
1219 footprints.

1220

1221 **Laser pulse (pulse for short).** Individual pulses of light emitted from the ATLAS laser are
1222 called laser pulses. As the pulse passes through the ATLAS transmit optics, this single pulse is
1223 split into 6 individual transmit pulses by the diffractive optical element. The 6 pulses travel to
1224 the earth's surface (assuming ATLAS is pointed to the earth's surface). Some attributes of a laser
1225 pulse are the wavelength, pulse shape and duration. Not: transmit pulse, laser shot, laser fire.

1226

1227 **Laser Beam.** The sequential laser pulses emitted from the ATLAS instrument that illuminate
1228 spots on the earth's surface are called laser beams. ATLAS generates 6 laser beams. The laser
1229 beam numbering convention follows the ATLAS instrument convention with strong beams
1230 numbered 1, 3, and 5 and weak beams numbered 2, 4, and 6 as shown in the figures. Not:
1231 beamlet.

1232

1233 **Transmit Pulse.** Individual pulses of light emitted from the ICESat-2 observatory are called
1234 transmit pulses. The ATLAS instrument generates 6 transmit pulses of light from a single laser
1235 pulse. The transmit pulses generate 6 spots where the laser light illuminates the surface of the
1236 earth. Some attributes of a given transmit pulse are the wavelength, the shape, and the energy.
1237 Some attributes of the 6 transmit pulses may be different. Not: laser fire, shot, laser shot, laser
1238 pulse.

1239

1240 **Reflected Pulse.** Individual transmit pulses reflected off the surface of the earth and viewed by
1241 the ATLAS telescope are called reflected pulses. For a given transmit pulse, there may or may
1242 not be a reflected pulse. Not: received pulse, returned pulse.

1243

1244 **Photon Event.** Some of the energy in a reflected pulse passes through the ATLAS receiver
1245 optics and electronics. ATLAS detects and time tags some fraction of the photons that make up
1246 the reflected pulse, as well as background photons due to sunlight or instrument noise. Any
1247 photon that is time tagged by the ATLAS instrument is called a photon event, regardless of
1248 source. Not: received photon, detected photon.

1249

1250 **Reference Ground Track (RGT).** The reference ground track (RGT) is the track on the earth at
1251 which a specified unit vector within the observatory is pointed. Under nominal operating
1252 conditions, there will be no data collected along the RGT, as the RGT is spanned by GT2L and
1253 GT2R (which are not shown in the figures, but are similar to the GTs that are shown). During
1254 spacecraft slews or off pointing, it is possible that ground tracks may intersect the RGT. The
1255 precise unit vector has not yet been defined. The ICESat-2 mission has 1387 RGTs, numbered
1256 from 0001xx to 1387xx. The last two digits refer to the cycle number. Not: ground tracks, paths,
1257 sub-satellite track.

1258

1259 **Cycle Number.** Over 91 days, each of the 1387 RGTs will be targeted in the Polar Regions
1260 once. In subsequent 91-day periods, these RGTs will be targeted again. The cycle number
1261 tracks the number of 91-day periods that have elapsed since the ICESat-2 observatory entered the
1262 science orbit. The first 91-day cycle is numbered 01; the second 91-day cycle is 02, and so on.
1263 At the end of the first 3 years of operations, we expect the cycle number to be 12. The cycle
1264 number will be carried in the mid-latitudes, though the same RGTs will (in general) not be
1265 targeted more than once.

1266

1267 **Sub-satellite Track (SST).** The sub-satellite track (SST) is the time-ordered series of latitude
1268 and longitude points at the geodetic nadir of the ICESat-2 observatory. In order to protect the
1269 ATLAS detectors from damage due to specular returns, and the natural variation of the position
1270 of the observatory with respect to the RGT throughout the orbit, the SST is generally not the
1271 same as the RGT. Not: reference ground track, ground track.

1272

1273 **Ground Tracks (GT).** As ICESat-2 orbits the earths, sequential transmit pulses illuminate six
1274 ground tracks on the surface of the earth. The track width is approximately 10m wide. Each
1275 ground track is numbered, according to the laser spot number that generates a given ground
1276 track. Ground tracks are therefore always numbered with 1L on the far left of the spot pattern
1277 and 3R on the far right of the spot pattern. Not: tracks, paths, reference ground tracks, footpaths.

1278

1279 **Reference Pair Track (RPT).** The reference pair track is the imaginary line halfway between
1280 the planned locations of the strong and weak ground tracks that make up a pair. There are three
1281 RPTs: RPT1 is spanned by GT1L and GT1R, RPT2 is spanned by GT2L and GT2R (and may be
1282 coincident with the RGT at times), and RPT3 is spanned by GT3L and GT3R. Note that this is

1283 the planned location of the midway point between GTs. We will not know this location very
1284 precisely prior to launch. Not: tracks, paths, reference ground tracks, footpaths, pair tracks.

1285

1286 **Pair Track (PT).** The pair track is the imaginary line half way between the actual locations of
1287 the strong and weak ground tracks that make up a pair. There are three PTs: PT1 is spanned by
1288 GT1L and GT1R, PT2 is spanned by GT2L and GT2R (and may be coincident with the RGT at
1289 times), and PT3 is spanned by GT3L and GT3R. Note that this is the actual location of the
1290 midway point between GTs, and will be defined by the actual location of the GTs. Not: tracks,
1291 paths, reference ground tracks, footpaths, reference pair tracks.

1292

1293 **Pairs.** When considered together, individual strong and weak ground tracks form a pair. For
1294 example, GT2L and GT2R form the central pair of the array. The pairs are numbered 1 through
1295 3: Pair 1 is comprised of GT1L and GT1R, pair 2 is comprised of GT2L and GT2R, and pair 3 is
1296 comprised of GT3L and 3R.

1297

1298 **Along-track.** The direction of travel of the ICESat-2 observatory in the orbit frame is defined as
1299 the along-track coordinate, and is denoted as the +x direction. The positive x direction is
1300 therefore along the Earth-Centered Earth-Fixed velocity vector of the observatory. Each pair has
1301 a unique coordinate system, with the +x direction aligned with the Reference Pair Tracks.

1302

1303 **Across-track.** The across-track coordinate is y and is positive to the left, with the origins at the
1304 Reference Pair Tracks.

1305

1306 **Segment.** An along-track span (or aggregation) of PE data from a single ground track or other
1307 defined track is called a segment. A segment can be measured as a time duration (e.g. from the
1308 time of the first PE to the time of the last PE), as a distance (e.g. the distance between the
1309 location of the first and last PEs), or as an accumulation of a desired number of photons.
1310 Segments can be as short or as long as desired.

1311

1312 **Signal Photon.** Any photon event that an algorithm determines to be part of the reflected pulse.

1313

1314 **Background Photon.** Any photon event that is not classified as a signal photon is classified as a
1315 background photon. Background photons could be due to noise in the ATLAS instrument (e.g.
1316 stray light, or detector dark counts), sunlight, or mis-classified signal photons. Not: noise
1317 photon.

1318

1319 **h_{**}**. Signal photons will be used by higher-level products to determine height above the
1320 WGS-84 reference ellipsoid, using a semi-major axis (equatorial radius) of 6378137m and a
1321 flattening of 1/298.257223563. This can be abbreviated as ‘ellipsoidal height’ or ‘height above
1322 ellipsoid’. These heights are denoted by h; the subscript ** will refer to the specific algorithm
1323 used to determine that elevation (e.g. is = ice sheet algorithm, si = sea ice algorithm, etc...). Not:
1324 elevation.

1325

1326 **Photon Cloud**. The collection of all telemetered photon time tags in a given segment is the (or
1327 a) photon cloud. Not: point cloud.

1328

1329 **Background Count Rate**. The number of background photons in a given time span is the
1330 background count rate. Therefore a value of the background count rate requires a segment of PEs
1331 and an algorithm to distinguish signal and background photons. Not: Noise rate, background
1332 rate.

1333

1334 **Noise Count Rate**. The rate at which the ATLAS instrument receives photons in the absence of
1335 any light entering the ATLAS telescope or receiver optics. The noise count rate includes PEs
1336 due to detector dark counts or stray light from within the instrument. Not: noise rate,
1337 background rate, and background count rate.

1338

1339 **Telemetry band**. The subset of PEs selected by the science algorithm on board ATLAS to be
1340 telemetered to the ground is called the telemetry band. The width of the telemetry band is a
1341 function of the signal to noise ratio of the data (calculated by the science algorithm onboard
1342 ATLAS), the location on the earth (e.g. ocean, land, sea ice, etc...), and the roughness of the
1343 terrain, among other parameters. The widths of telemetry bands are adjustable on-orbit. The
1344 telemetry bandwidth is described in Section 7 or the ATLAS Flight Science Receiver Algorithms
1345 document. The total volume of telemetered photon events must meet the data volume constraint
1346 (currently 577 GBits/day).

1347

1348 **Window, Window Width, Window Duration**. A subset of the telemetry band of PEs is called a
1349 window. If the vertical extent of a window is defined in terms of distance, the window is said to
1350 have a width. If the vertical extent of a window is defined in terms of time, the window is said to
1351 have a duration. The window width is always less than or equal to the telemetry band.

1352

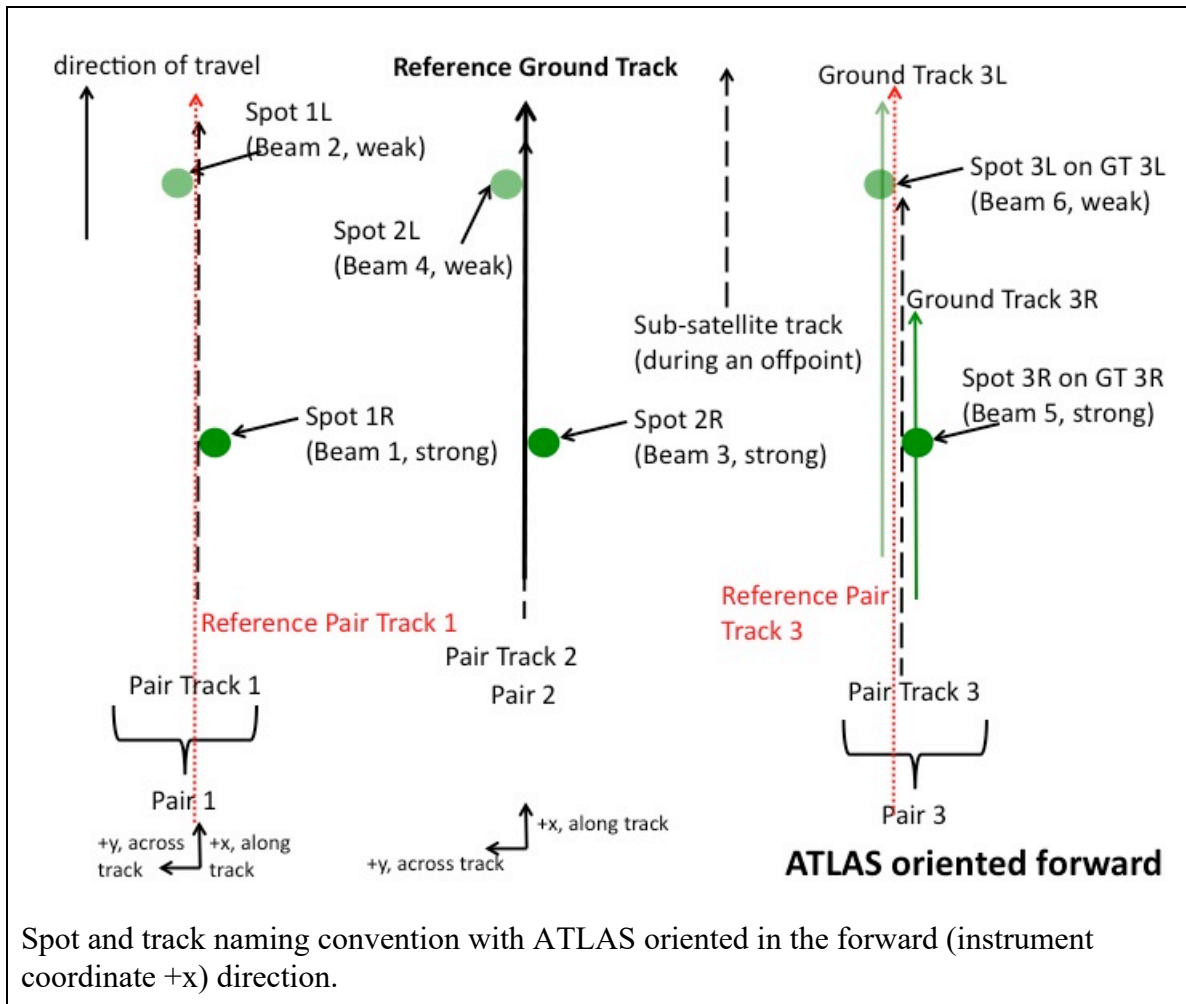
1353

1354

1355

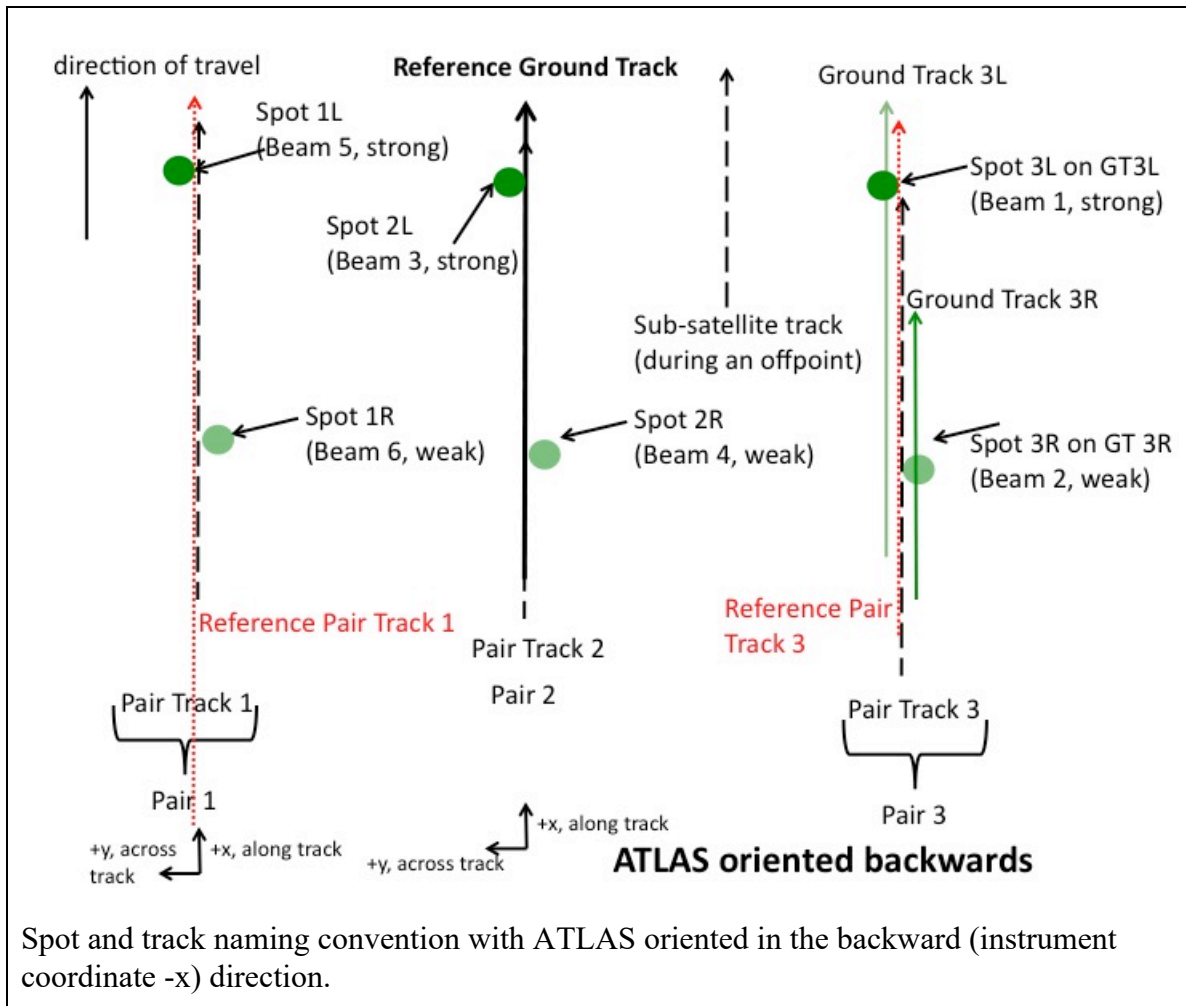
1356

Figure 6-1. Spots and tracks, forward flight



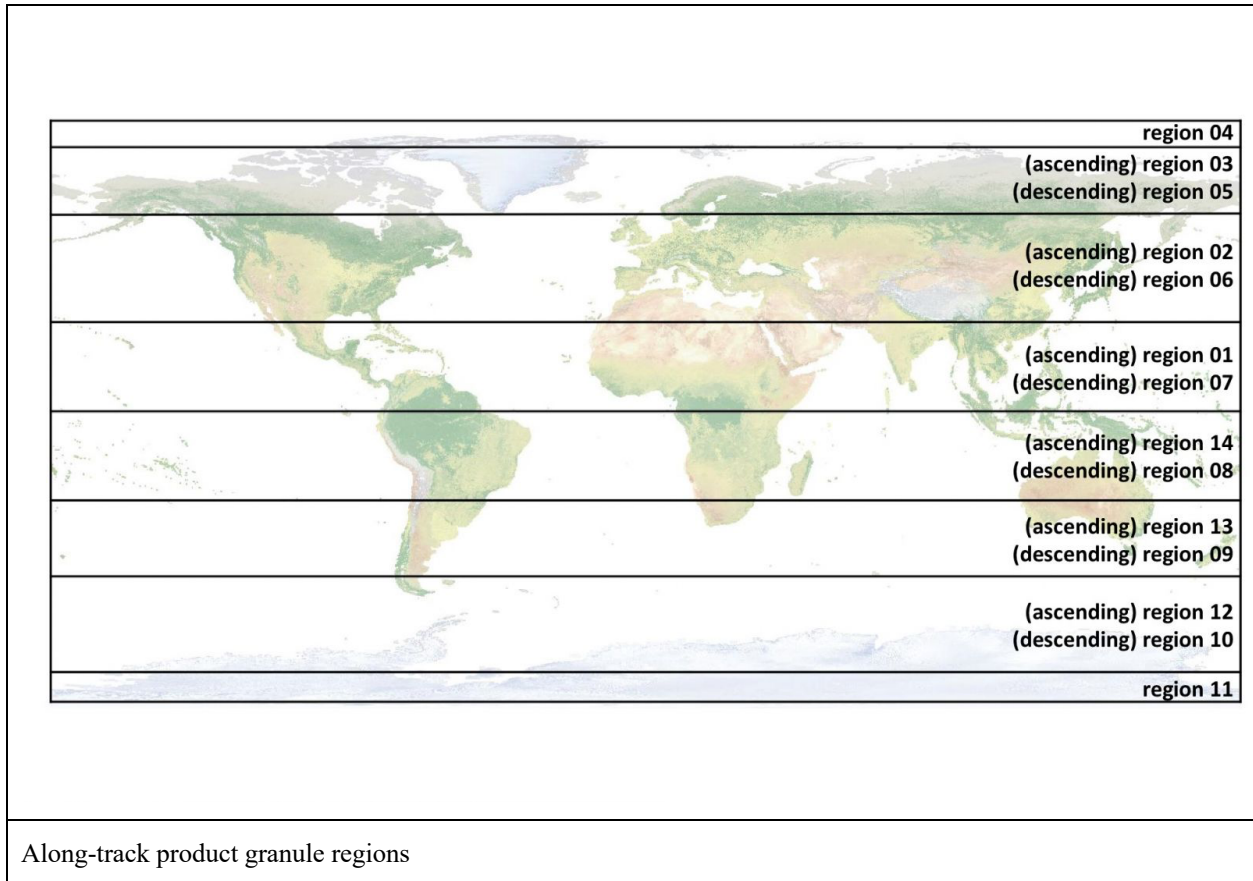
1357
 1358
 1359
 1360
 1361
 1362
 1363
 1364
 1365
 1366

Figure 6-2. Spots and tracks, backward flight



1367

Figure 6-3. Granule regions



1368 **7.0 BROWSE PRODUCTS**

1369 For each ATL11 data file, there will be eight figures written to an associated browse file. Two of
 1370 these figures are required and are located in the default group; default1 and default2. The browse
 1371 filename has the same pattern as the data filename, namely,
 1372 ATL11_tttss_c1c2_rr_vVVV_BRW.h5, where tttt is the reference ground track, ss is the orbital
 1373 segment, c1 is the first cycle of data in the file, c2 is the last cycle of data in the file, rr is the
 1374 release and VVV is the version. Optionally, the figures can also be written to a pdf file.

1375

1376 Below is a discussion of the how the figures are made, with examples from the data file
 1377 ATL11_009403_0307_02_vU07.h5. Note that the figure numbering in this section is distinct
 1378 from that in the rest of the document; the figures shown here are labeled as they are in each
 1379 browse-product file.

1380

1381

1382

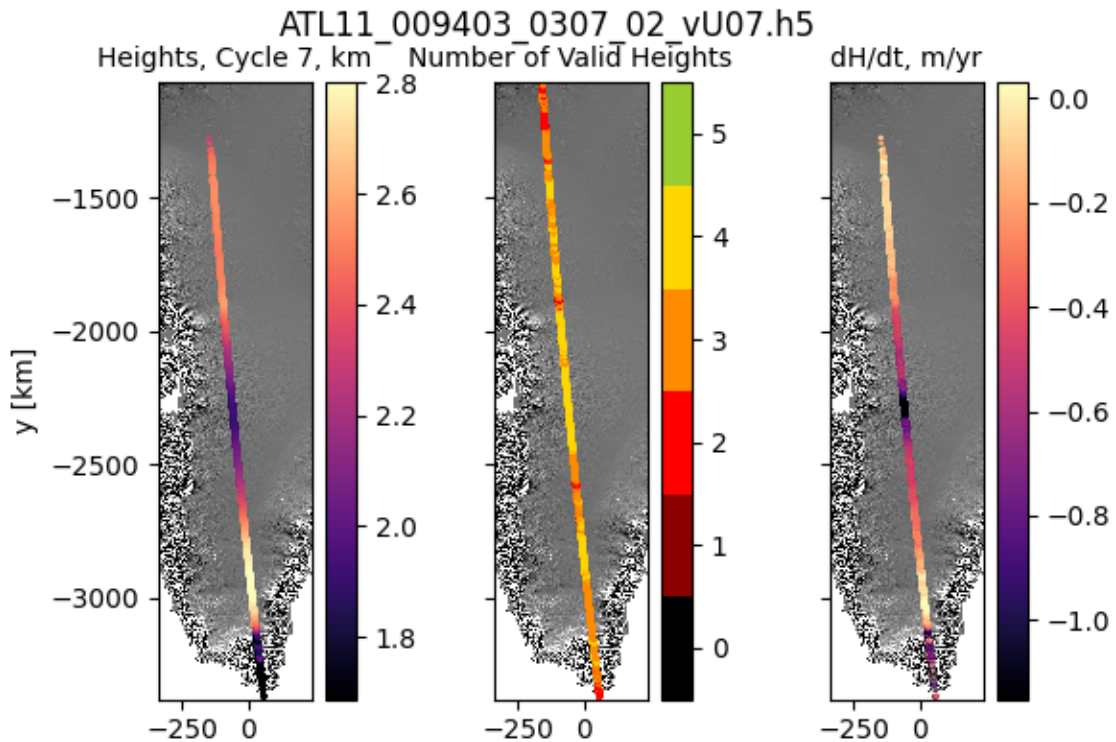


Figure 1. Height data, in km, from cycle 7 (1st panel). Number of cycles with valid height data (2nd panel). Change in height over time, in meters/year, cycle 7 from cycle 3 (3rd panel). All overlaid on gradient of DEM. x, y in km. Maps are plotted in a polar-stereographic projection with a central longitude of 45W and a standard latitude of 70N.

1383

1384

1385 The background for the three panels in Figure 1 is the gradient DEM in gray scale. It is shown in
 1386 a polar-stereographic projection with a central longitude of 45W (0E) and a standard latitude of
 1387 70N (71S), for the Northern (Southern) Hemisphere. The map is bounded by the extent of height
 1388 data plus a buffer. ATL11 heights (/ptx/h_corr) from all pairs of the latest cycle with valid data,
 1389 here cycle 7, are plotted in the first panel. The “magma” color map indicates the heights in km.
 1390 The limits on the color bar are set with the python scipy.stat.scoreatpercentile method at 5% and
 1391 95%. In the second panel are plotted the number of valid heights summed over all cycles at each
 1392 location. The color bar extends to the total number of cycles in the data file. The change in height
 1393 over time, dH/dt, is plotted in the third panel, in meters/year. dHdt is the change in height of the
 1394 last cycle with valid data from the first cycle with valid data (/ptx/h_corr) divided by the
 1395 associated times (/ptx/delta_time). Text of ‘No Data’ is printed in the panel if there is only one
 1396 cycle with valid data, or if the first and last cycles with valid data have no common reference
 1397 point numbers (/ptx/ref_pt). All plots are in x,y coordinates, in km. This figure is called
 1398 default/default1 in the BRW.h5 file.

1399

ATL11_009403_0307_02_vU07.h5

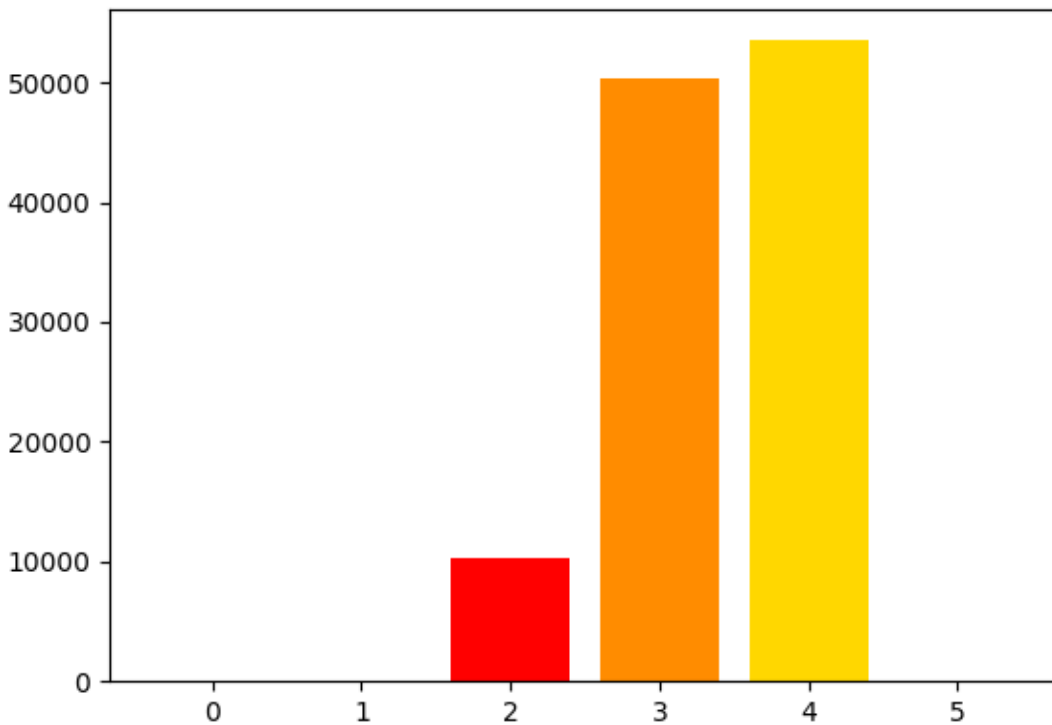


Figure 2. Histogram of number of cycles with valid height measurements, all beam pairs.

1400

1401

1402 A histogram of the number of valid height measurements (/ptx/h_corr) is in Figure 2. Valid
 1403 height data are summed across all cycles, for each reference point number (/ptx/ref_pt). The
 1404 color scale is from zero to the total number of cycles in the data file and matches those in Figure
 1405 1, 2nd panel. This figure is called validrepeats_hist in the BRW.h5 file.

1406

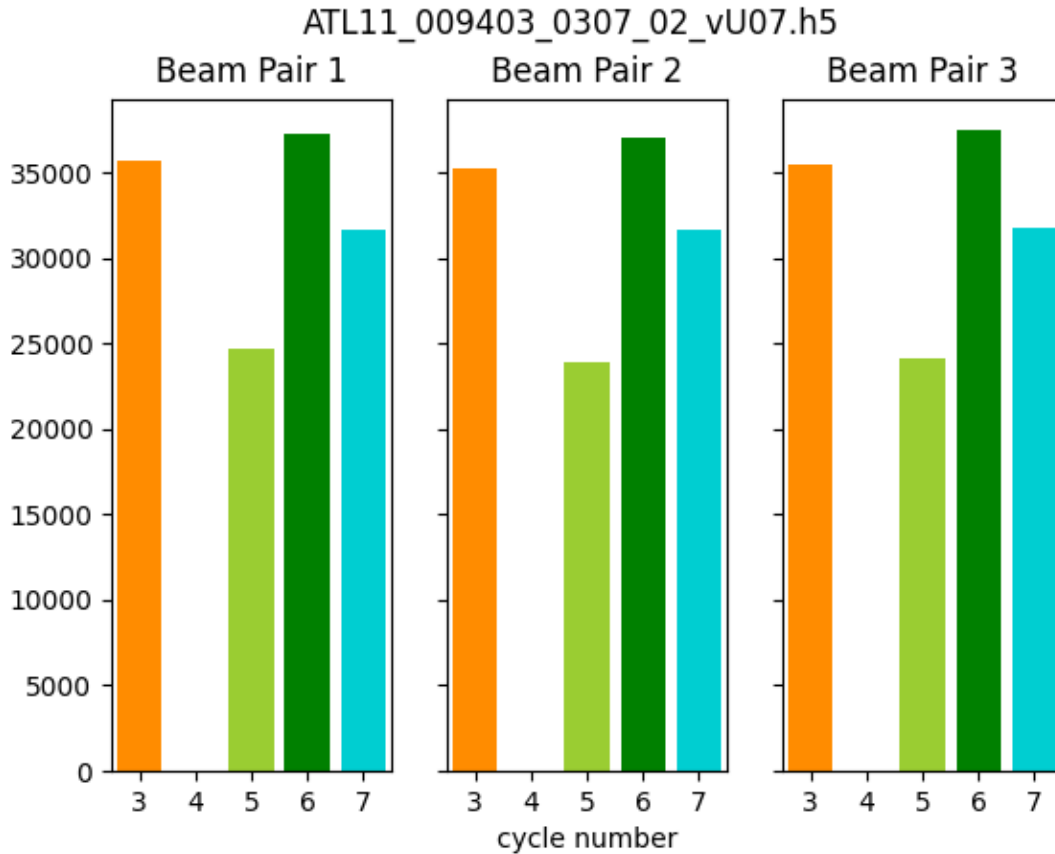


Figure 3. Number of valid height measurements from each beam pair.

1407

1408

1409 Histograms in Figure 3 show the number of valid heights (/ptx/h_corr) for each cycle, separated
 1410 by beam pair. The cycle numbers are color coded. This figure is called default/default2 in the
 1411 BRW.h5 file.

1412

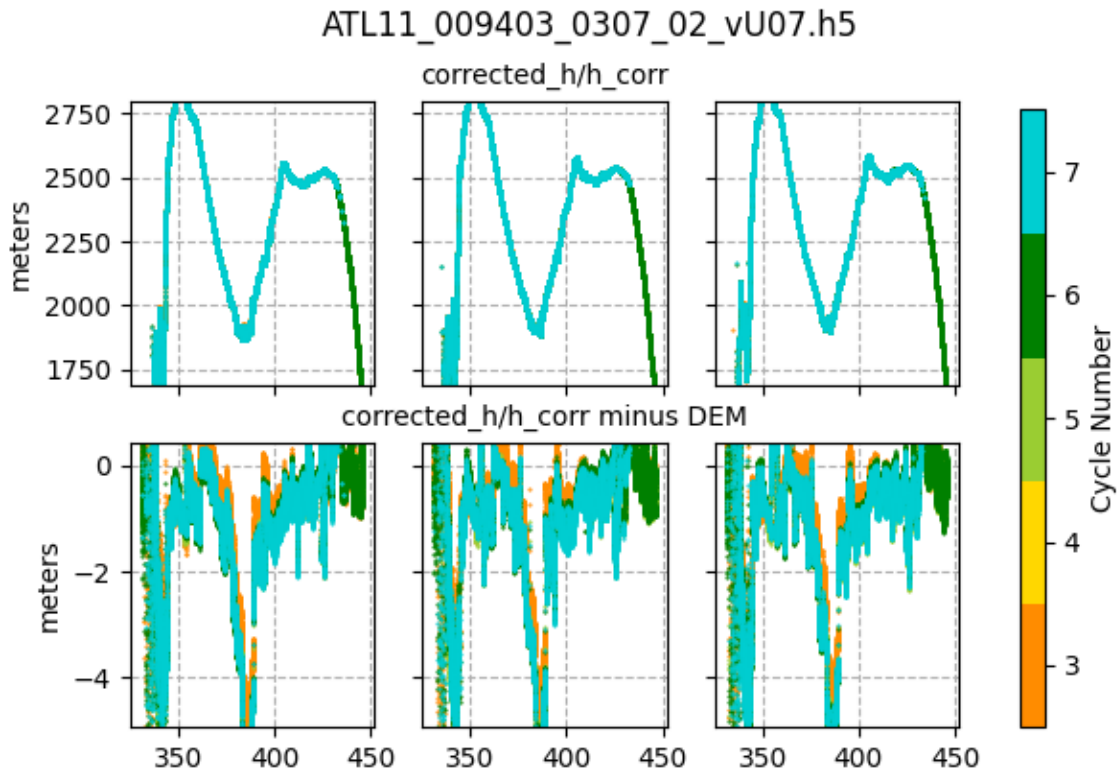


Figure 4. Top row: Heights, in meters, plotted for each beam pair: 1 (left), 2 (center), 3 (right). Bottom row: Heights minus DEM, in meters. Y-axis limits are scores at 5% and 95%. Color coded by cycle number. Plotted against reference point number/1000.

1413

1414

1415 There are six panels in Figure 4, with two rows and three columns. In the top row are plotted the
 1416 height measurements (/ptx/h_corr) for each beam pair, one pair per panel. In the bottom row are
 1417 plotted the same height measurements minus the collocated DEM (ref_surf/dem_h) values, one
 1418 pair per panel. The plots are color coded by cycle number, as in Figure 3. The heights are plotted
 1419 versus reference point number (/ptx/ref_pt) divided by 1000 for a cleaner plot. The y-axis is in
 1420 meters for both rows. The y-axis limits for the top and bottom rows are set separately, using the
 1421 python scipy.stats.scoreatpercentile method with limits of 5% and 95% for heights and height
 1422 differences, respectively. Text of 'No Data' is printed in a panel if there are no valid height data
 1423 for that pair. This figure is called h_corr_h_corr-DEM in the BRW.h5 file.

1424

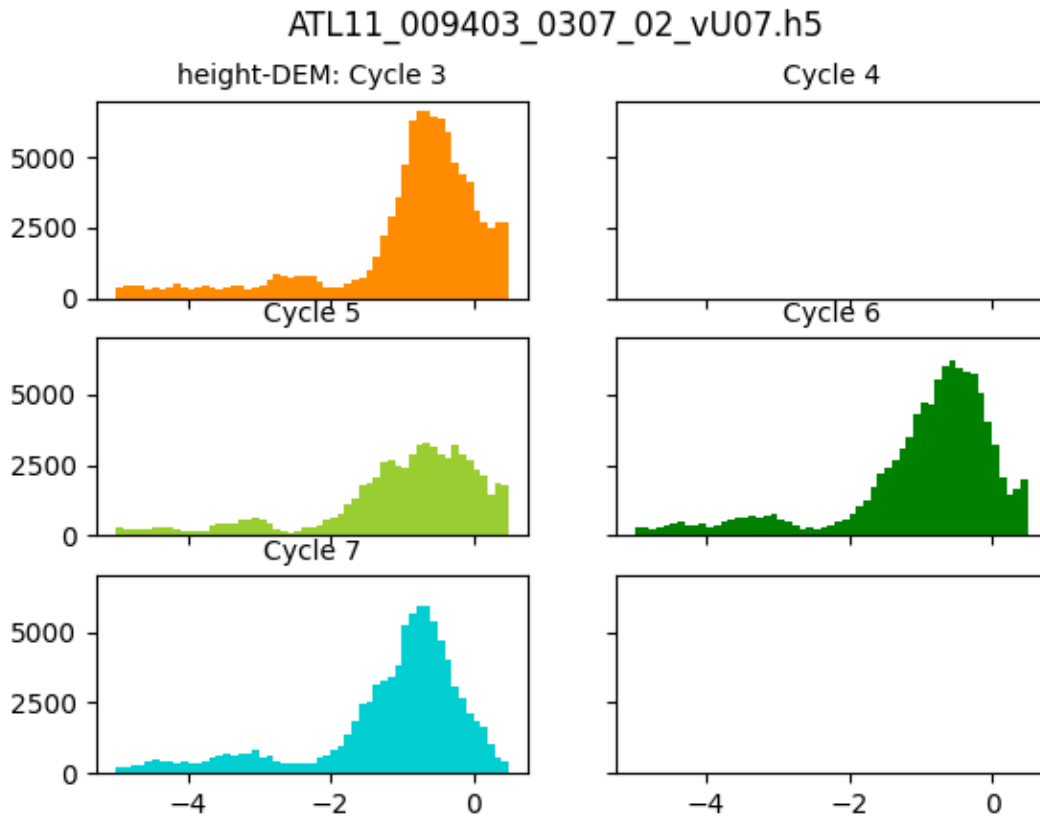


Figure 5. Histograms of heights minus DEM heights, in meters. One histogram per cycle, all beam pairs. X-axis limits are the scores at 5% and 95%.

1425

1426

1427 Figure 5 is associated with Figure 4. It is a multi-paneled figure, with the number of panels
 1428 dependent on the number of cycles in the data file. Each panel is a histogram of the heights
 1429 (/ptx/h_corr) minus collocated DEM heights (ref_surf/dem_h) color coded by cycle, the same as
 1430 in Figures 3 and 4. The limits on the histograms are set using the python
 1431 scipy.stats.scoreatpercentile method with limits of 5 and 95% for all cycles of data, the same
 1432 values used in Figure 4 bottom row. This figure is called h_corr-DEM_hist in the BRW.h5 file.

1433

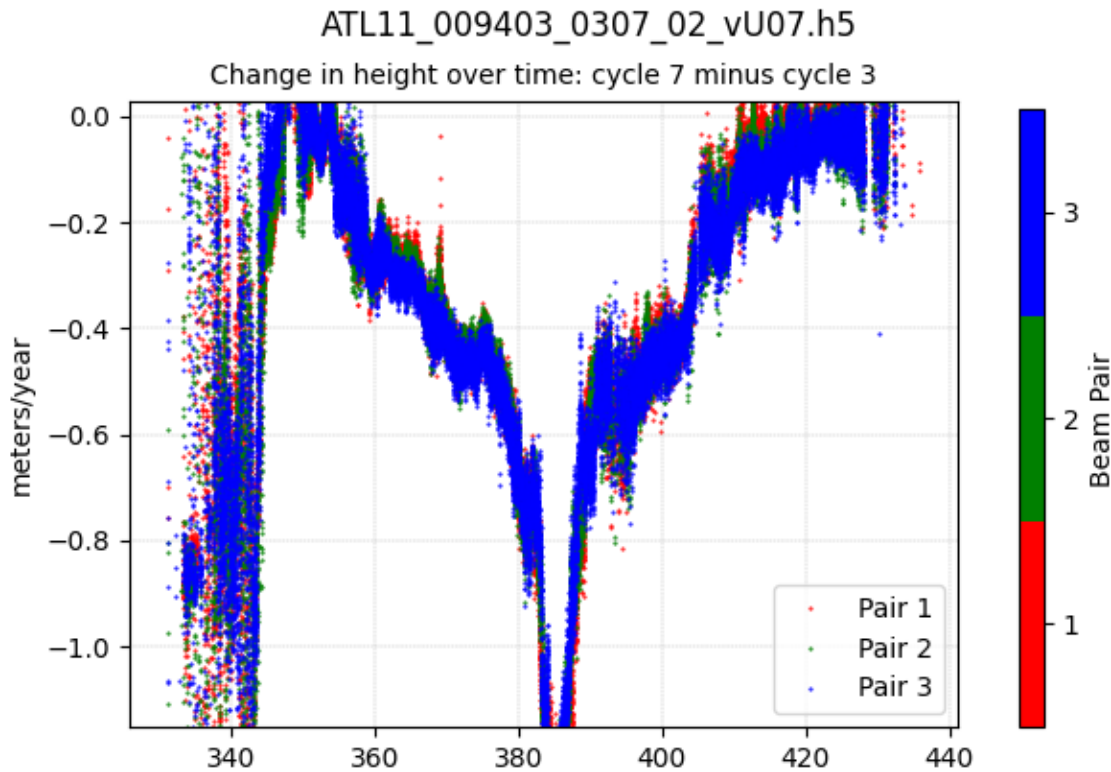


Figure 6. Change in height over time, dH/dt , in meters/year. dH/dt is cycle 7 from cycle 3. Color coded by beam pair: 1 (red), 2 (green), 3 (blue). Y-axis limits are scores at 5% and 95%. Plotted against reference point number/1000.

1434

1435

1436 The changes in height with time, dH/dt , in meters/year are plotted in Figure 6. The calculation
 1437 differences the first and last cycles with valid height data ($/ptx/h_corr$) divided by the associated
 1438 time differences ($/ptx/delta_time$). The change in heights for pair 1 are in red, for pair 2 are in
 1439 green and for pair 3 are in blue. The y-axis limits are set using the python
 1440 `scipy.stats.scoreatpercentile` method with limits of 5% and 95%. The x-axis is reference point
 1441 number ($/ptx/ref_pt$) divided by 1000 for a cleaner plot. Text of 'No Data' is printed in the panel
 1442 if there is only one cycle with valid data, or if the first and last cycles with valid data have no
 1443 common reference point numbers. This figure is called $dHdt$ in the BRW.h5 file.

1444

1445

1446

Glossary/Acronyms

ASAS	ATLAS Science Algorithm Software
ATBD	Algorithm Theoretical Basis Document
ATLAS	ATLAS Advance Topographic Laser Altimeter System
CDF	Cumulative Distribution Function
DEM	Digital Elevation Model
GSFC	Goddard Space Flight Center
GTs	Ground Tracks
ICESat-2	Ice, Cloud, and Land Elevation Satellite-2
IKR	I Know, Right?
MABEL	Multiple altimeter Beam Experimental Lidar
MIS	Management Information System
NASA	National Aeronautics and Space Administration
PE	Photon Event
POD	Precision Orbit Determination
PPD	Precision Pointing Determination
PRD	Precise Range Determination
PSO	ICESat-2 Project Science Office
PTs	Pair Tracks
RDE	Robust Dispersion Estimate
RGT	Reference Ground Track
RMS	Root Mean Square
RPTs	Reference Pair Tracks

ICESat-2 Algorithm Theoretical Basis Document (ATBD) for Land Ice H(t) (ATL11)

Release 001

RT	Real Time
SCoRe	Signature Controlled Request
SIPS	ICESat-2 Science Investigator-led Processing System
TLDR	Too Long, Didn't Read
TBD	To Be Determined

1447

References

1448 Brunt, K.M., H.A. Fricker and L. Padman 2011. Analysis of ice plains of the Filchner-Ronne Ice
1449 Shelf, Antarctica, using ICESat laser altimetry. *Journal of Glaciology*, **57**(205): 965-975.

1450 Fricker, H.A., T. Scambos, R. Bindshadler and L. Padman 2007. An active subglacial water
1451 system in West Antarctica mapped from space. *Science*, **315**(5818): 1544-1548.

1452 Schenk, T. and B. Csatho 2012. A New Methodology for Detecting Ice Sheet Surface Elevation
1453 Changes From Laser Altimetry Data. *Ieee Transactions on Geoscience and Remote Sensing*,
1454 **50**(9): 3302-3316.

1455 Smith, B., H.A. Fricker, N. Holschuh, A.S. Gardner, S. Adusumilli, K.M. Brunt, B. Csatho, K.
1456 Harbeck, A. Huth, T. Neumann, J. Nilsson and M.R. Siegfried 2019a. Land ice height-retrieval
1457 algorithm for NASA's ICESat-2 photon-counting laser altimeter. *Remote Sensing of*
1458 *Environment*: 111352.

1459 Smith, B.E., H.A. Fricker, I.R. Joughin and S. Tulaczyk 2009. An inventory of active subglacial
1460 lakes in Antarctica detected by ICESat (2003-2008). *Journal of Glaciology*, **55**(192): 573-595.

1461 Smith, B.E., D. Hancock, K. Harbeck, L. Roberts, T. Neumann, K. Brunt, H. Fricker, A.
1462 Gardner, M. Siegfried, S. Adusumilli, B. Csatho, N. Holschuh, J. Nilsson and F. Paolo 2019b.
1463 Algorithm Theoretical Basis Document for Land-Ice Along-track Product (ATL06). Goddard
1464 Space Flight Center.

1465